AN ABSTRACT OF THE THESIS OF

<u>Johannes L. Eggers</u>   for the   <u>M.S.</u>   in   <u>E.E.</u>
     (Name)   (Degree)   (Major)

Date thesis is presented <u>July 10, 1964</u>

Title <u>Percussion Welding Force, Temperature, and Time</u>

<u>Relationships for</u> Welding 6061-T6 Aluminum

Abstract approved   Redacted for Privacy
                         (Major professor)

The force, temperature, and time relationships were investigated by using oscilloscope measurement techniques. Force was measured using a strain gage and the dynamic response recorded with a polaroid oscilloscope camera. Temperature was measured with a tungsten-rhenium thermo-couple and recorded in the same manner. Residual stress measurements were made to determine an approximate temperature gradient of the weld zone. Tensile strength was used for determining the quality of the weld. All relationships were displayed using tensile strength as the dependent variable.

An exponentially-shaped drop shaft was designed to control the force characteristics. No force wave-reflections were observed. The design criteria were high damping, smooth transitions, and coupling to the air.

Process variables were reduced to allow observation of the force, time, and temperature relationships. The magnetic field, due to the current carrying leads, was a

major factor in causing unsymmetrical arc formation and was reduced by shielding. Resistance of the circuit was controlled by providing bolted connections and using stainless steel strips for the variable resistance element. The voltage and capacitance parameters were maintained at one setting in order to eliminate their effect. Oxide layers were not controlled but the studs and plates were cleaned of grease and films.

Metallurgical relationships are discussed but not displayed. Cracking in the weld zone exists in some cases and overaging has been observed. These adverse metallurgical effects usually accompany a thick weld zone.

PERCUSSION WELDING FORCE, TEMPERATURE

AND TIME RELATIONSHIPS FOR WELDING

6061-T6 ALUMINUM

by

Johannes Lyle Eggers

A THESIS

submitted to

OREGON STATE UNIVERSITY

in partial fulfillment of
the requirements for the
degree of

Master of Science

September, 1964

APPROVED:

Assistant Professor of Electrical Engineering

In Charge of Major

Head of Electrical Engineering

Dean of Graduate School

Date thesis is presented _July 10, 1964_

Typed by Erma McClanathan

ACKNOWLEDGMENTS

TABLE OF CONTENTS

Percussion Welding Force, Temperature and Time Relationships for Welding 6061-T6 Aluminum

INTRODUCTION

The American Society for Metals defines percussion welding as "An electric-resistance butt-welding process in which the weld area is upset or forged at the moment of welding" (2, p. 10). The energy for welding is stored in capacitors, and released in an arc as the stud (in this case) approaches the plate at constant velocity. After the stud makes physical contact with the plate the percussive force forges the stud and plate surfaces together. The arc time is dependent on velocity, the stud tip, and the voltage of the charged capacitors. The melted material cools very rapidly due to the thermo-dynamic properties of the stud and plate. The equipment used and a welded stud are shown in Figure 1.

Previous work has been concentrated on many of the outside parameters such as capacitance, voltage, resist-ance, force and velocity. Assumptions pertaining to temperature relationships are generally quite vague due to the speed and high temperatures of the process. Thermo-dynamic studies are not feasible due to the removal of heat energy when the percussive force pushes molten metal out of the weld zone. Various stud shapes and platings have been previously investigated. A more complete

Figure 1 a
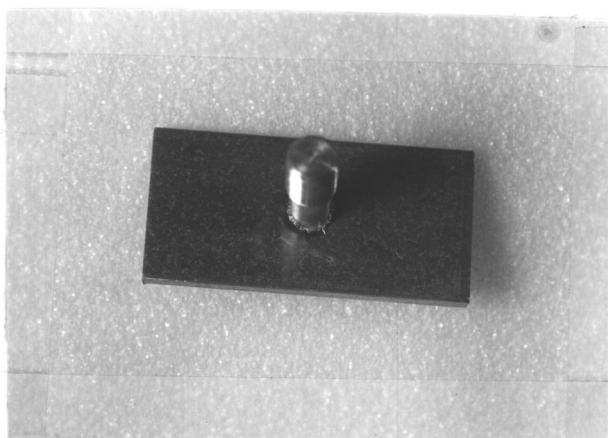
Figure 1 b

Figure 1:   a)   The equipment used

b)   A welded stud

summary of previous work is available in the bibliography articles, but it is evident that new methods of attack are desirable.

OBJECTIVE OF FORCE, TEMPERATURE, AND TIME RELATIONSHIPS

Utilizing force, temperature, and time relationships, the number of parameters are reduced to force and temperature as a function of time. The quantity of variables requires either a multivariable analysis or fixation of several variables and multiple analysis. Both approaches are laborious and require the use of a large computer, which is generally not available to manufacturers or users of percussive welders.

Force, temperature, and time relationships are basic to the percussion welding process. In aluminum welding, overaging results if the temperature is held too high for too long a period. In general, diffusion of alloying elements destroy the characteristics of the alloy. The percussive force determines the amount of molten metal pushed out of the weld zone and provides filling of voids. In attempting to determine other variables during solidification of the weld zone, only the current and the material characteristics are apparent. The current will affect the temperature a negligible amount, since heat conduction away from the weld zone is very rapid.

The relationships are easy to measure and record.
Transient temperature and force measurements are possible
using standard oscilloscope techniques. No publications
covering force, temperature, and time relationships have
been found in the literature. Comstock had used a slow
response (30 mil diameter) low melting point (Chromel-
Alumel) thermocouple and obtained the temperature measure-
ment below 1300 degrees centigrade. Transient force
measurements are quite common and have been used in many
applications including percussive welding (20, p. 35).

PROCESS VARIABLES AND THEIR CONTROL

The percussion welding process has well-defined
variables and hidden variables. The hidden variables are
functions of the well-defined. The magnetic field, cir-
cuit resistance, and stud alignment are three important
variables that were minimized in this case.

The magnetic field was found to cause an unsymmetri-
cal weld during the preparations for Comstock's factorial
data run. A large quantity of mild steel was used to
shield the weld area from the magnetic fields as shown
in Figure 2, p. 5. The amount of mild steel was chosen
to eliminate the unsymmetrical welds. Electrical steel
-M6 (4, p. 788) was obtained later and it was found that
only one-third of the cross-sectional area was necessary
to eliminate unsymmetrical welds.
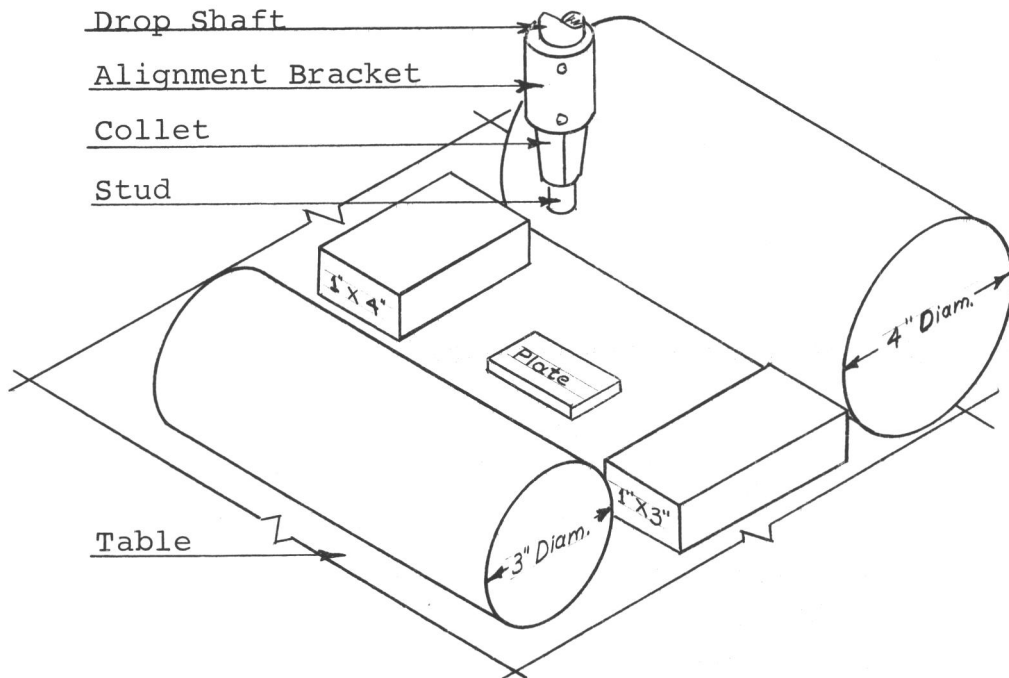
Figure 2.   Magnetic shielding
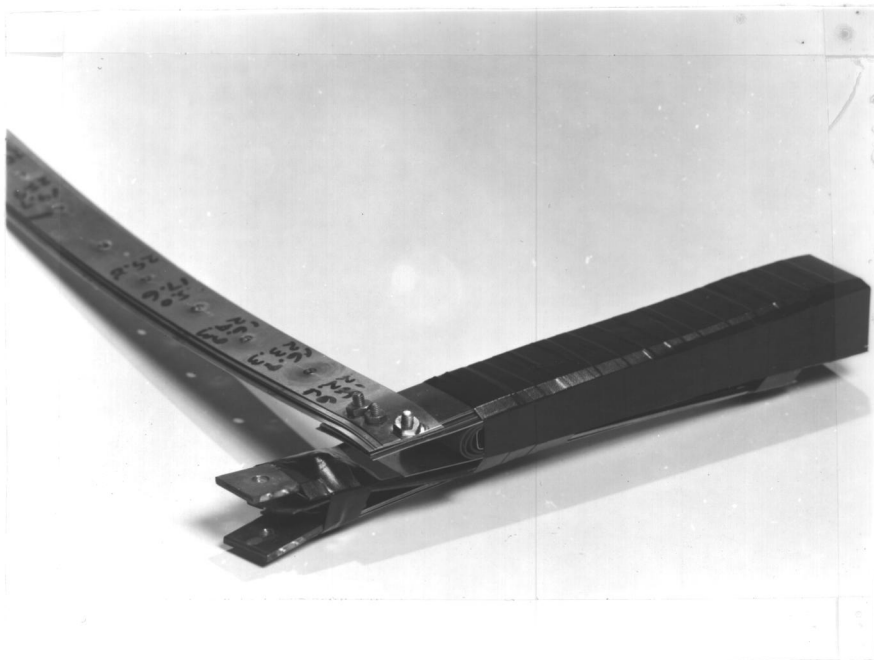
Figure 3.   Stainless steel resistor

The resistance of the circuit is hard to control
since the circuit resistance is between three and 40
milliohms. Circuit connections must be maintained at a
high contact pressure in order to eliminate a variable
resistance characteristic. During preparation for Com-
stock's factorial data run, a copper-to-aluminum junction
failed twice, therefore the section of aluminum bus was
replaced with copper. Aluminum-to-copper connections must
be isolated from the atmosphere or galvanic corrosion will
take place (2, p. 895). The resistance between the stud
holding collet and the stud was minimized by keeping the
collet pressure fairly high. One aid in this case is that
the aluminum oxide layer on the stud threads is removed
when sliding the stud into the collet. Even with high
collet pressures evidence of heat dissipated at the
junction was observed in the form of aluminum melting onto
the collet. The resistance of the plate to the work table
is dependent on clamping pressure on the plate, the oxide
layer on the plate and the cleanliness of the table. A
clamping force of 60 pounds through two clamping fingers,
each one-half inch diameter, was necessary to maintain
the clamping resistance within 0.05 milliohms.

A stainless steel strip (68 mils thick by one inch
wide) with holes drilled to give steps of approximately
one-half milliohm was used to vary resistance (see Figure 3

p. 5). By measuring the resistance before and after
welding, 50 percent of the measurements varied by less
than .1 milliohm and the maximum difference recorded was
.71 milliohm (using a sample size of 40 welds).

The oxide layer on aluminum results in the arc taking
the path of least resistance and can cause an unsymmetrical
weld. An analogous effect was displayed by placing electri-
cal tape across one-fourth the weld area. The same is true
of oil films that may exist on the metal (2, p. 779-786).
The oil films were removed by cleaning the plate and stud
with paper towel soaked with paint thinner. Consideration
was given to removing the oxide layer with an alkaline
substance, but the distortion of the surface would then
become a problem. The stud must be perpendicular to the
plate or this will also cause an unsymmetrical weld. In
this case the arc propagates to the two closest points on
one side of the stud.

The process variables were real and were controlled to
produce consistently good welds. The magnetic field effect
was the most pronounced cause of consistently unsymmetrical
welds with oxide layers causing an occasional unsymmetrical
weld. These process variables were reduced to allow
investigation of the force, temperature, and time relation-
ships.

OSCILLOSCOPE MEASUREMENTS

The temperature sensing element was a 26 percent
Rhenium-Tungsten versus a five percent Rhenium-Tungsten
thermocouple. This material is manufactured by The Hoskins
Manufacturing Company. Temperature versus emf data is in
the appendix on page 52. The formation of the thermocouple
bead was performed by using the circuit of Figure 4. The
hardware used is shown in Figure 5. The two thermocouple
elements were twisted together for about one-fourth inch
and connected to the resistor. The capacitors were charged
to 50 volts and the end of the thermocouple quickly touched
against the carbon block to form a bead as shown in Figure
6, p. 11. The bead is quite brittle since the tungsten was
heated above 2000° F. The other ends of the thermocouple
element were wrapped and soldered directly to a shielded,
twisted-pair cable. The thermocouple was placed directly in
the weld zone as shown in Figure 7, p. 11.

The thermocouple wire was selected five mils diameter
on the basis of rise time and physical size. The rise time
was calculated to be less than ten microseconds which is
100 times less than the arc time (14, p. 65-67). The
strength of the thermocouple was considered in conjunction
with rise time and approximately 50 percent of the measure-
ments were failures due to breakage of the wires. A larger
thermocouple wire would provide more strength, but would

50 Watt - 3 Ohm Resistor

Alligator Clip

Thermocouple

50 volts

77,500 Microfarads

Carbon Block 1-1/2"x1-1/2" x 1/4"

Alligator Clip
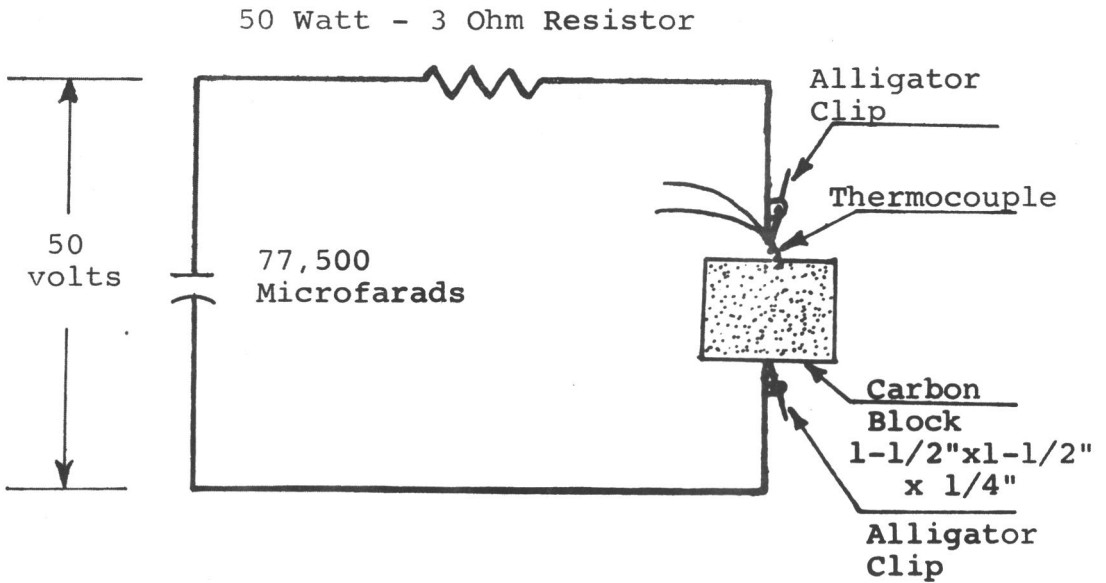
Figure 4.   Circuit diagram for thermocouple bead formation
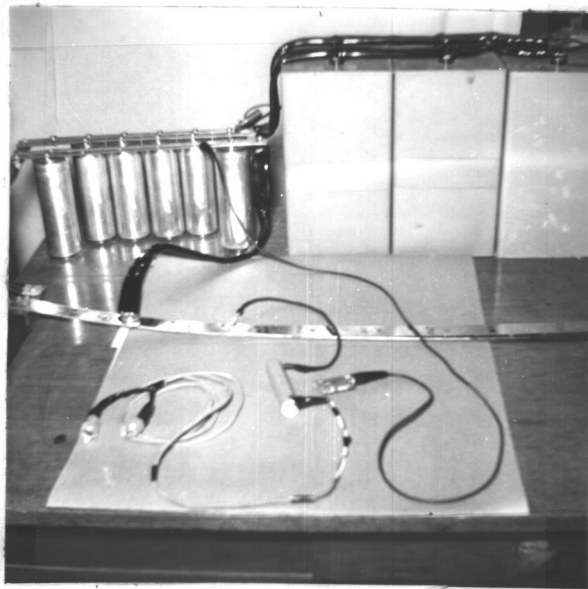
Figure 5.   Hardware for thermocouple bead formation

interfere with the weld process, and result in a
greater response time.

A shielded-twisted-pair cable was selected to con-
nect the thermocouple to the oscilloscope. The cable
length was five feet and attenuation was negligible.
The shielding was connected to ground and the twisted
pair was connected to the differential amplifier (24).

The differential amplifier was selected for its
common mode rejection and its high cut-off frequency.
In the direct-current coupled condition, the common mode
rejection ratio is 10,000 to one. This allowed measure-
ment of the thermocouple emf when the thermocouple was
touching the stud at a potential of ten volts. The high
cut-off frequency (850 kilocycles per second) allowed
measurement of the temperature characteristics.

A typical temperature versus time trace is shown in
Figure 8 and the following terminology is used. Arc
time is the time characterized by loss of the tempera-
ture trace until the temperature becomes stable. Arc
time temperatures are near the vaporization temperature
of aluminum. Freeze time is the period between arc time
and the decreased cooling rate. Freeze time temperatures
are between the vaporization temperature and the freeze
point temperature.

The force measurements were obtained by using strain
gages on the drop shaft and on the stud. The strain gages
were applied on opposite sides of the drop shaft and of
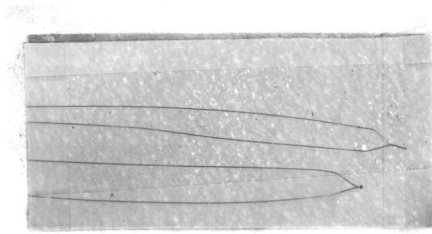
Figure 6.   Thermocouple
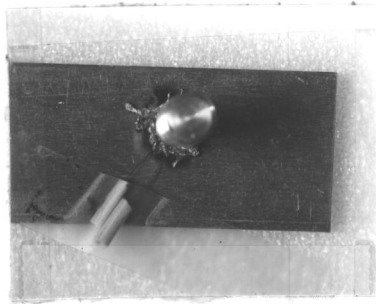
Figure 7.   Thermocouple after welding

10 millivolts
per centimeter

5 milliseconds per centimeter
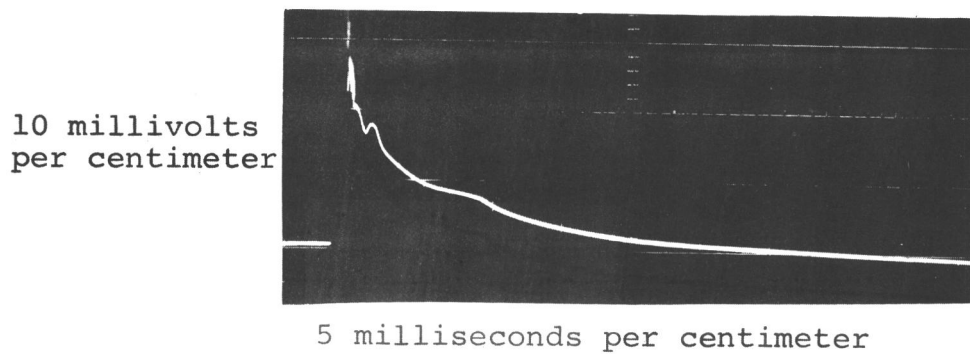
Figure 8.   Temperature versus time oscilloscope trace

the stud to cancel bending strains. The strain gages on the drop shaft were connected to minimize inductive pickup and located above the drop-shaft alignment bracket. They were Baldwin-Lima-Hamilton SR4 foil strain gages type HFA with a gage factor of $2.2^{+}.1$ and resistance of $113.8^{+}.2$ ohms. They were applied with Eastman 910 cement and encapsulated with "Duco" cement. The stud strain gages were never used during the welding process. The stud strain gages were of the same manufacturer but of the formed wire variety, Type AF-7-1 with a gage factor of $2.00^{+}2$ percent and resistance of $119.0^{+}.3$ ohms. These were applied using fast drying SR4 cement and encapsulated with "Duco" cement.

The strain gages were calibrated and the calibration curves are shown in Figure 9, p. 13. A universal testing machine (see Figure 21, p. 27) was used to provide and measure the calibrating force. The resistance of the strain gages was measured with a model 291 "ESI" bridge. The type HFA strain gage, and the strain gages mounted on the stud are shown in Figure 10, p. 14.

The interconnection between the strain gages and the oscilloscope was a shielded twisted-pair cable. The cable length was eight feet and attenuation was negligible. The shielding was connected to ground and the twisted-pair was connected between the strain gage and the differential amplifier. The circuit diagram is shown in Figure 11, p. 15.
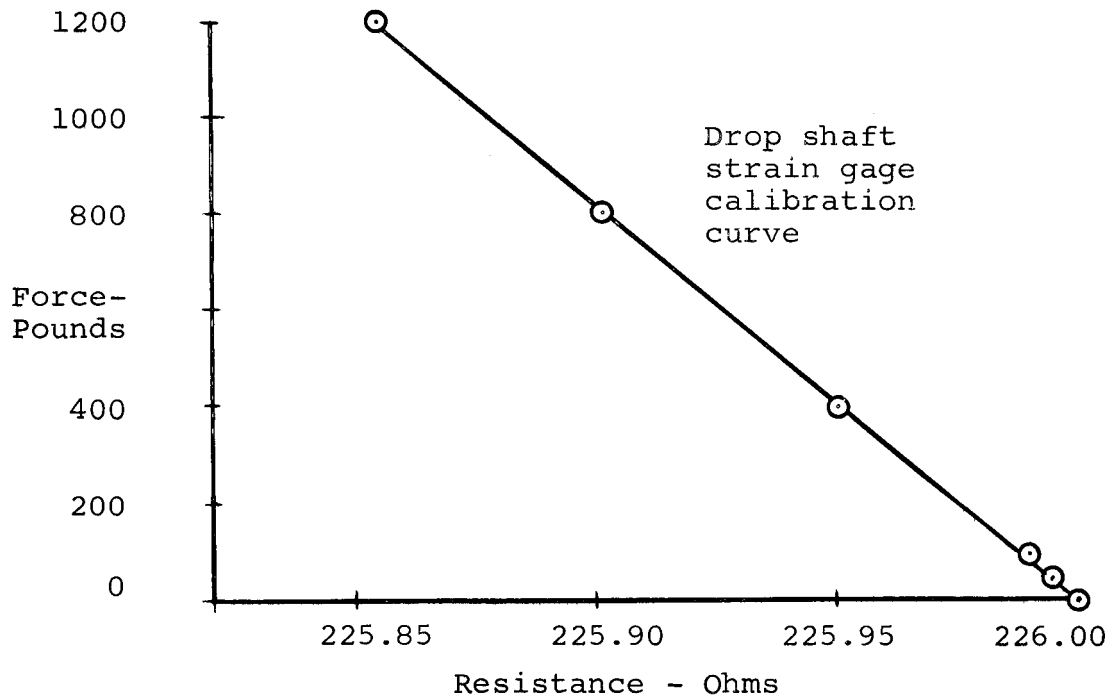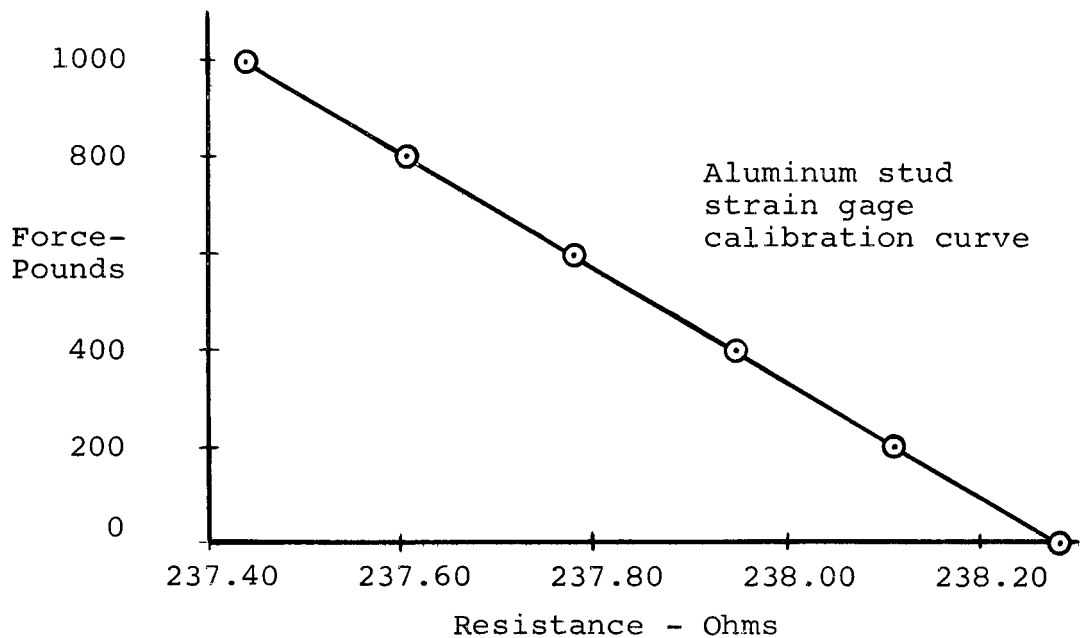
Figure 9. Strain gage calibration curves
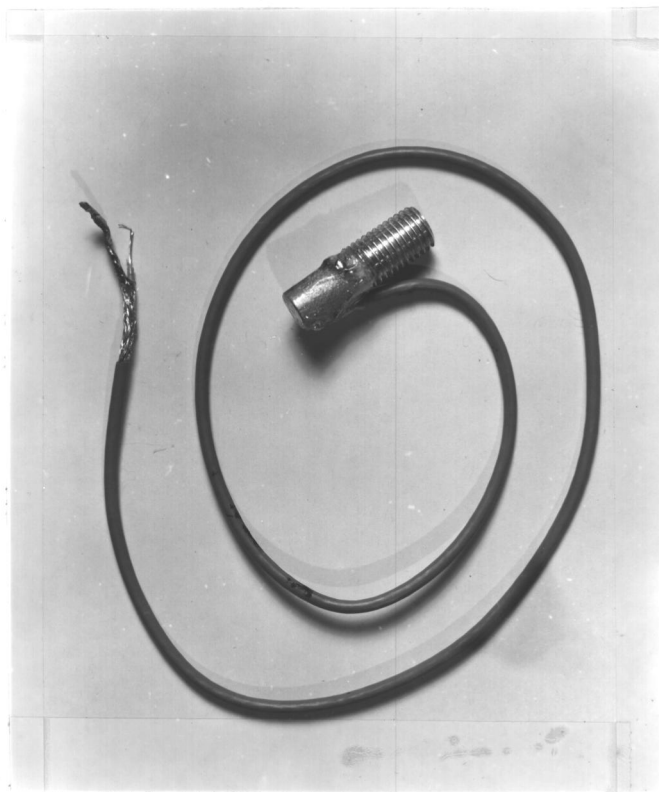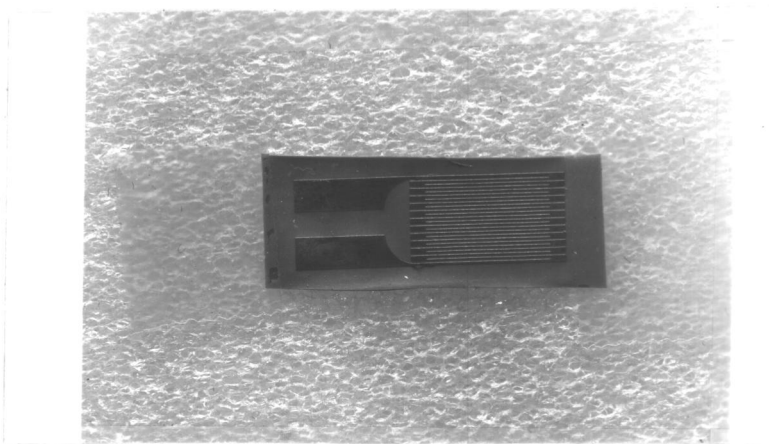
Figure 10.   Top: Type HFA strain gage

              Bottom: Stud mounted type A-F-7-1
                         strain gages
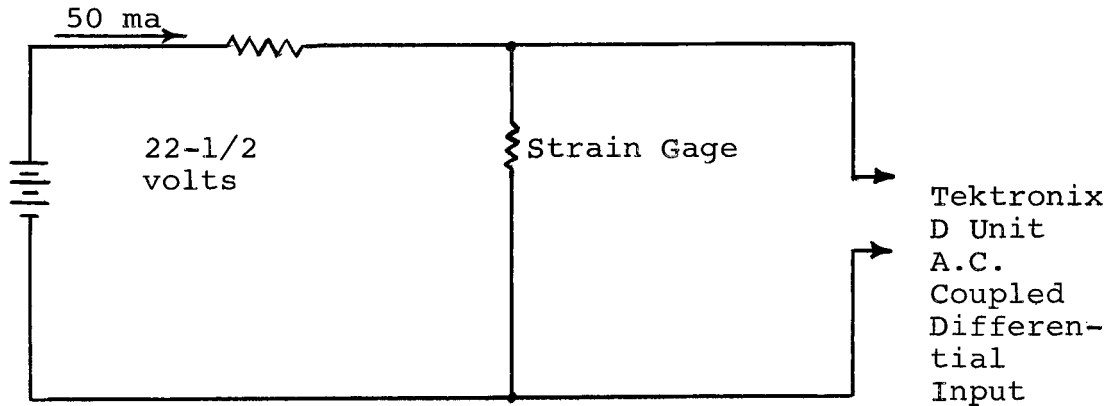
Figure 11.   Force Measurement Circuit Diagram

The strain-gage response time was calculated from measurements of the shunt capacitance, and the resistance to ground was measured. The shunt capacitance of the strain gage with the measurement cable attached was found to be 900 picofarads. The rise time is simply the product of resistance and capacitance and for the drop shaft meas- urement system was calculated to be 200 nanoseconds. Since the stud strain gages are much smaller, the shunt capaci- tance will be less, and the rise time will be less. The resistance between the shaft (or stud) and the strain gages was measured and found to be greater than thirty megohms.

The differential amplifier was in the AC coupled position for the force measurements. In this coupling con- dition the common mode rejection ratio is reduced to 600 to one which doesn't constitute a problem since the insulation to the shaft is 30 megohms. The cut-off frequency for

force measurements was 550 kilocycles per second at the sensitivity used.

A force versus time oscilloscope trace drawing is shown in Figure 12, p. 18. When the force starts, physical contact between the stud and plate exists and the arc is extinguished. The point where the force starts is the end of the arc time and the beginning of the freeze time. Some inductive pickup exists when the arc first starts and when the arc is extinguished.

The system circuit diagram is shown in Figure 13, p. 18. The oscilloscope was a Tektronix 551 dual beam. The triggering circuit was a model 108 Bourns potentiometer connected to a 22-1/2 volt battery with the "slider" serving as the triggering source. A battery was used to supply the strain gage current, since the ripple of standard power supplies caused 5 millivolts of noise. The major noise problem was due to ground loops and inductive pickup. The ground loops were eliminated by connecting the ground in a star fashion. Inductive pickup existed in the strain gage measurements even though connections were made in a cancellation manner. The force measurements were basically the same with or without welding. High frequency (100 megacycles) noise existed on the thermocouple during arc time.

RESISTANCE MEASUREMENTS

The circuit resistance was measured with a model 291 ESI bridge as shown in Figure 14. The leads of the discharge circuit (without the stainless steel resistor) were measured as 3.81 milliohms. Measurement of the lead's resistance, with 77,500 microfarads of electrolytic capacitors connected, was 3.87 milliohms. All resistance measurements were made with the capacitors connected in the circuit. The measurement leads were wrapped and soldered directly to the ends of the discharge-circuit leads. The measurement leads had a constant resistance which was subtracted from the bridge readings.

RESIDUAL STRESS MEASUREMENTS

Residual stress is defined as "Macroscopic stresses that are set up within a metal as the result of non-uniform plastic deformation. This deformation may be caused by cold working or by drastic gradients of temperature incurred by quenching or welding" (2, p. 12). They are sometimes called "locked-up" stresses (3, p. 89-96), and are caused by bending, plating, welding, forming, machining, shot peening, and almost all metallurgical treatments. There are many methods of detecting and measuring residual stresses, and they can be categorized into the three broad fields of chemical, lacquers, and
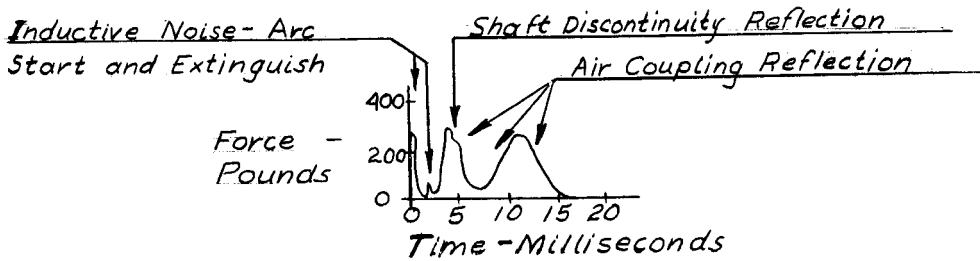
Figure 12. Force versus time oscilloscope trace drawing
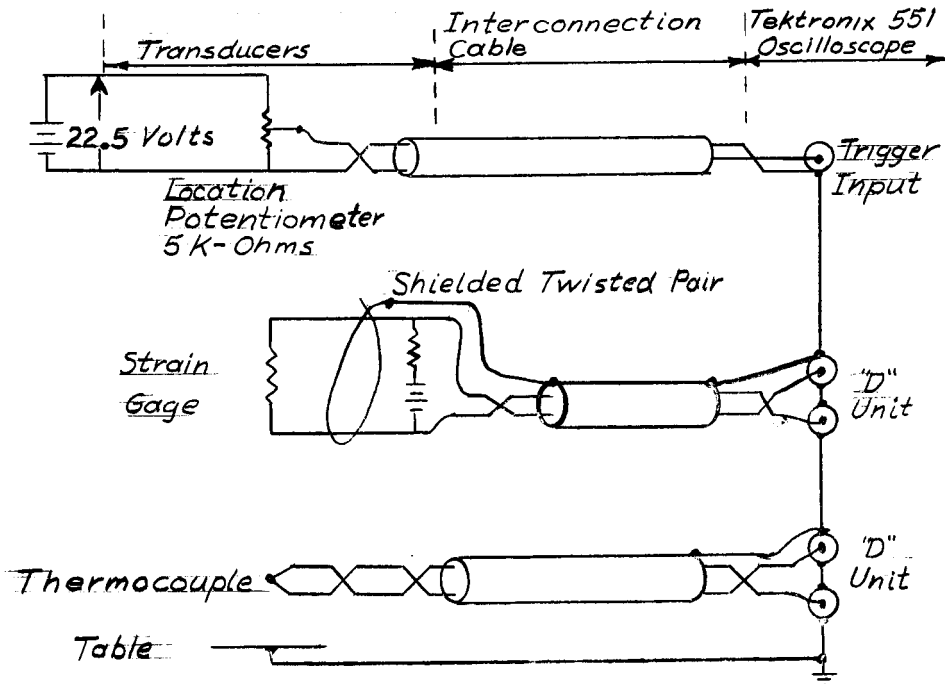

Figure 13. Measurement system circuit diagram
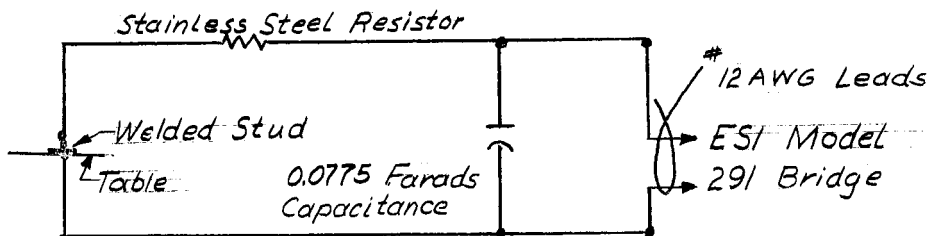
Figure 14. Resistance measuring circuit

mechanical. The chemical methods are qualitative and depend on the rate of reaction on stressed specimens. The lacquers are also qualitative, to a degree, depending on strain cracks in the lacquered surface upon stress relief. The mechanical methods are quantative and depend on measurements before and after stress relief.

The method of residual stress measurement was conceived to satisfy the tough requirements of percussive welding residual stress. Thermodynamic properties cause a temperature gradient which is generally hotter at the mass center of the weld zone. The temperature coefficient of expansion causes residual stresses. The stresses can be detected by length measurements taken before and after stress relief. The strains are related to stresses in accordance with Hookes Law (21, p. 43). The weld zone was quite thin (one-half to ten mils), therefore Saint Venants Principle (21, p. 42) was considered in determining how great an area should be investigated. An area approximately one-thirty-second of an inch on each side of the weld zone was investigated. The stress relief used was similar to the Kreitz method (3, p. 96).

Residual stress measurements were made by using the Tukon* tester to apply and measure a grid of microhardness

*Wilson Mechanical Instrument Company, Model L. R. Tukon Tester, Number Lr206.

indentations placed on a diametrical slice (see Figure 16, p. 22). The first specimen diametrical slice was prepared by removing 100 mils from one side and 100 mils from the other by wet grinding. The second specimen diametrical slice was prepared by alternately removing ten mils per side until one hundred mils were removed from each side. The general steps of preparation are shown in Figure 15, p. 21. Both grids were 19 columns by 11 rows of micro-hardness indentations as shown in Figure 17, p. 22. A microhardness indentation before and after stress relief is shown in Figure 18, p. 22. If the diametrical slice is too thick, three-dimensional residual stresses will cause deformation of the microhardness indentations upon stress relief. All measurements given are in terms of filar eye-piece units where one mil equals approximately 150 filar units (500X magnification).

The microhardness indentation spacing was measured five times over four arbitrarily chosen spaces identified as A, B, C, D. Then the mean value was computed for each spacing.

|	Space A	Space B	Space C	Space D
1st. Measurement	946	1004	1000	1019
2nd. Measurement	946	1003	1001	1017
3rd. Measurement	945	1003	1000	1019
4th. Measurement	944	1003	1001	1017
5th. Measurement	944	1002	999	1020
Mean Value	945	1003	1000.4	1018.4
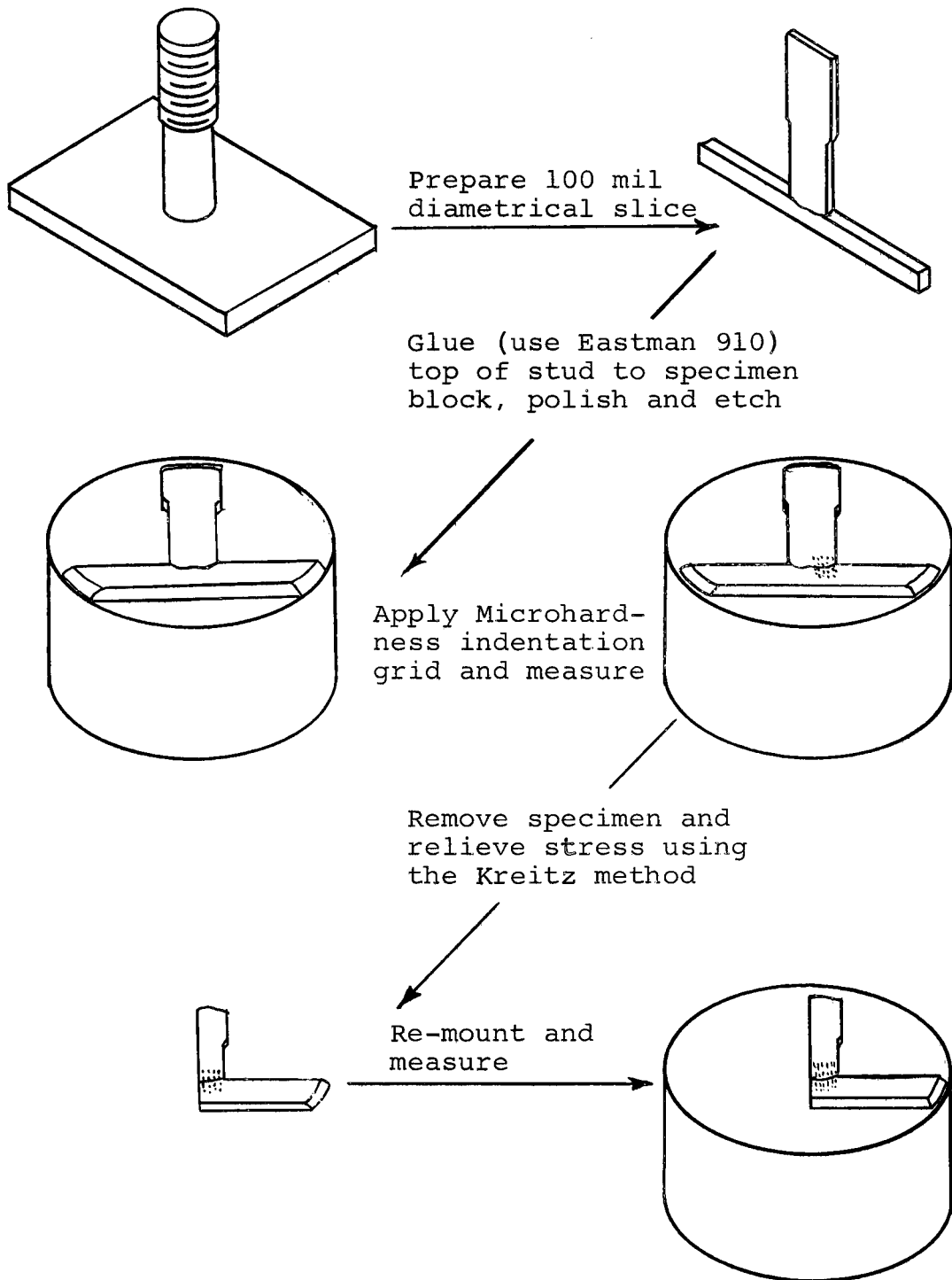
Figure 15.   Residual-stress specimen preparation

Figure 16.   Tukon tester
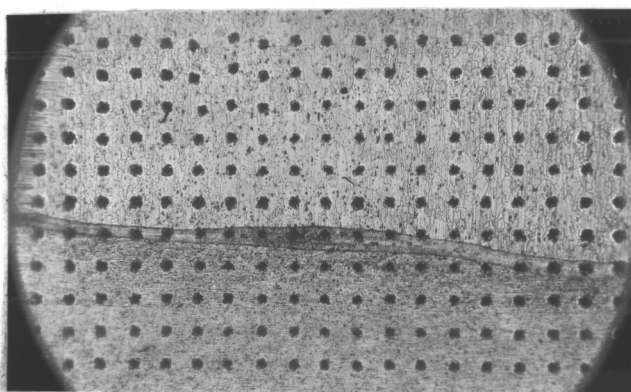
Figure 17.   Microhardness indentation pattern 25X
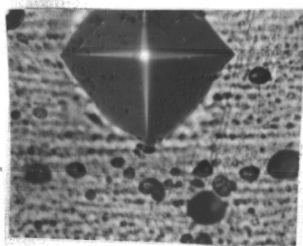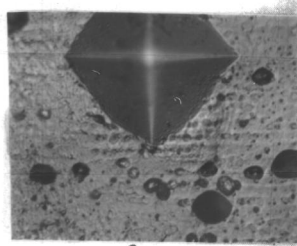
a.   b.

Figure 18.   A microhardness indentation a) before
              stress relief, b) after stress relief;
              note lack of change to microhardness
              indentation 500X

The error of each measurement is assumed to be the difference between each individual measurement and its mean. In order to remain on the conservative side the largest observed error, 1.6, was chosen. In any column of ten spaces the probable error would be the error of measurement times the square root of ten which equals approximately 5.06. Since the change in length involves two additions of ten measurements the error for strain calculations should be 5.06 times the square root of two, which equals 7.1.

The results of the residual stress calculations are shown in Figures 19 and 20. The data and calculations are in the appendix on page 53. The least squares approximation calculations are on page 54 in the appendix. A temperature difference between the center and the outside diameter (of the stud weld zone) was calculated to be 250 degrees Centigrade. The calculation was made by dividing the difference in strain (0.006) by the coefficient of thermal expansion (2.4×10^{-5}) (2, p. 822).

TENSILE STRENGTH MEASUREMENTS

The tensile strength of the welded specimens was measured on a *universal testing machine shown in

*Baldwin-Tate-Emery 60,000-lb. Universal Hydraulic Testing Machine.

Stress-
psi.

Strain-
in./in.

Location - Measurement Column Numbers

Weld Zone
Thickness-
Filar Eyepiece
Units (500X)

Location - Measurement Column Numbers
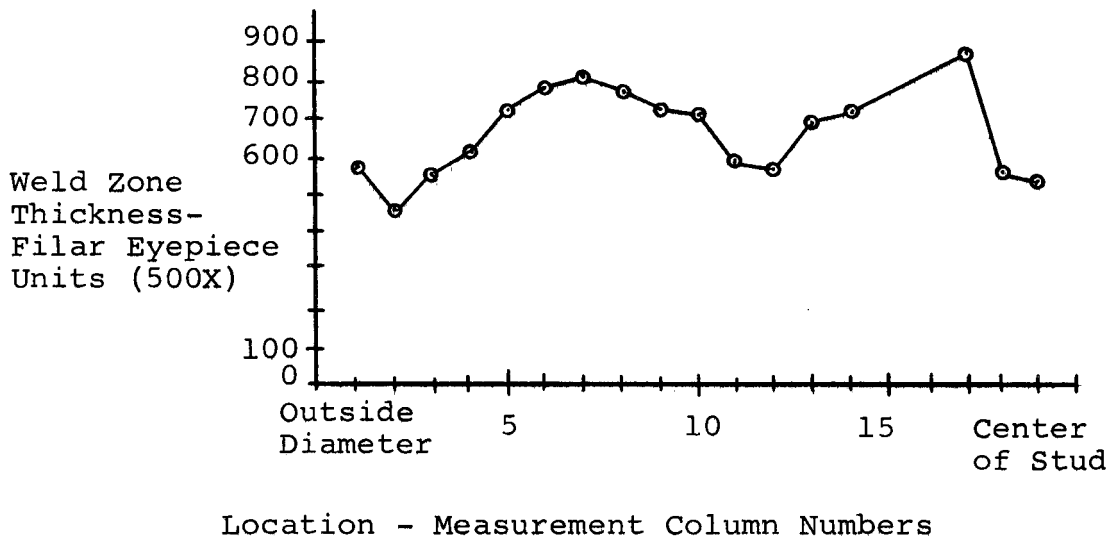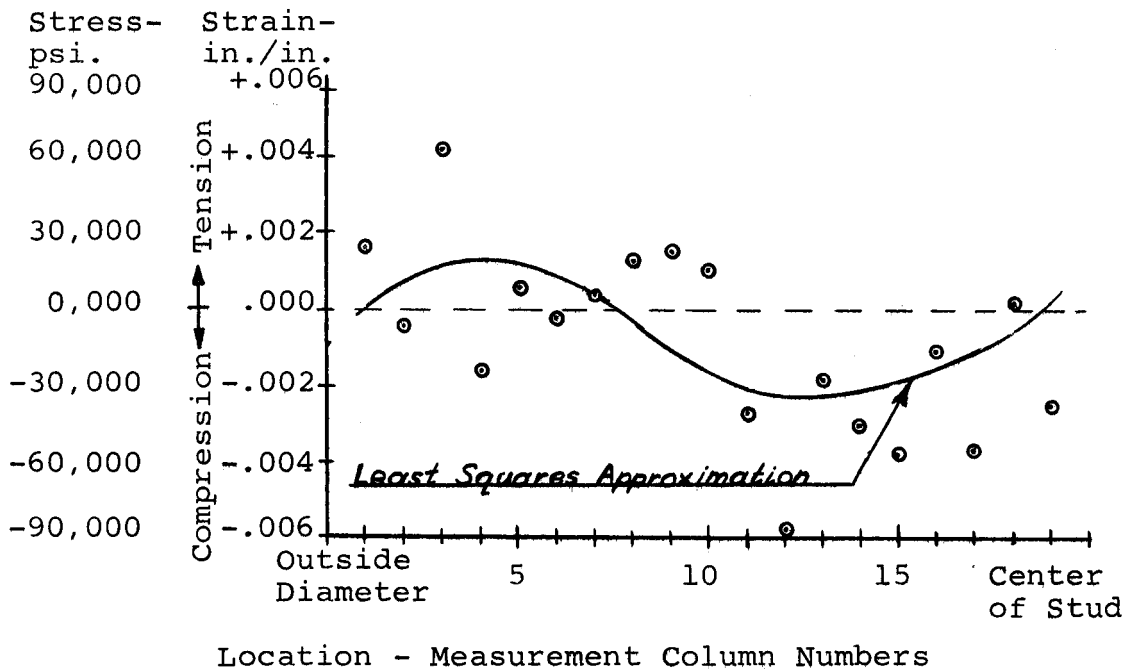
Figure 19. First specimen residual stress and weld
zone thickness curves
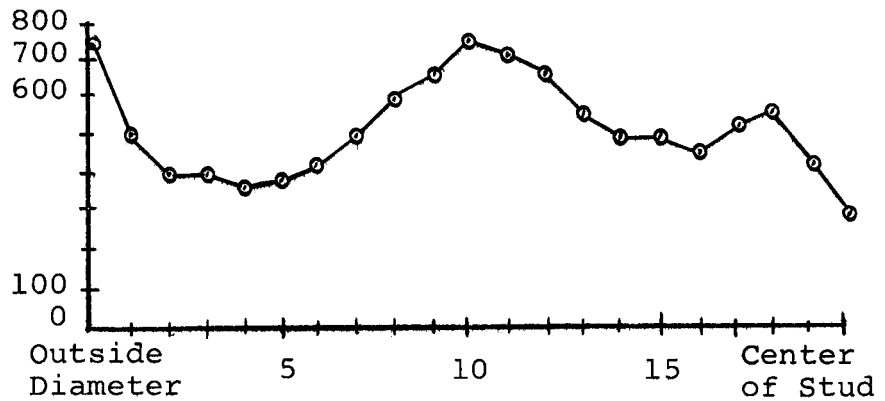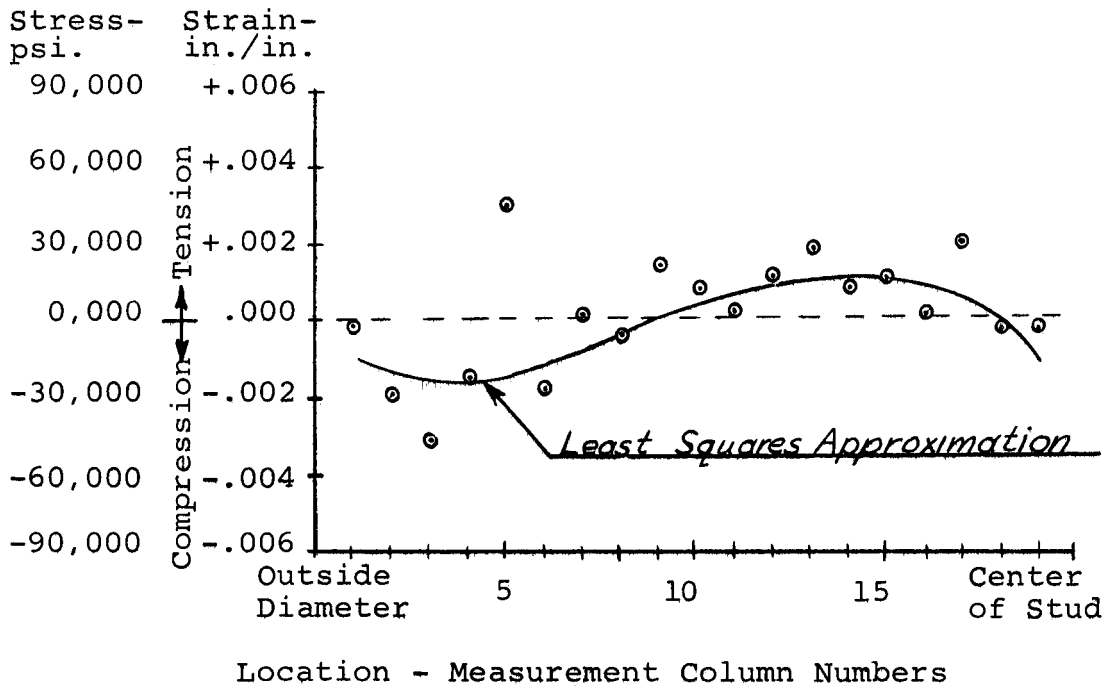
Figure 20.   Second specimen residual stress and weld
             zone thickness curves

Figure 21. The clamping fixture shown in Figure 22 was designed by Comstock and used to hold the specimen during the tensile test. All tensile testing used a constant loading rate of 1,000 pounds per minute as monitored by the R. F. Blanks loading rate device on a universal testing machine.

RESULTS OF ORIGINAL DROP SHAFT MEASUREMENTS

A series of force versus time measurements were made at varying drop heights as shown by the oscilloscope traces of Figure 23, p. 28. A second series of oscilloscope traces were made at various weights as shown in Figure 24, p. 29, 30.

The tensile strength versus resistance curve of Figure 25, p. 31 was for a specific force characteristic and setting all other parameters at a fixed level. Due to the multitude of force wave forms, the force wave of Figure 24b was chosen for further analysis. The capacitance and voltage were arbitrarily set at 77,500 microfarads and 150 volts respectively. The data is on page 57 of the appendix.
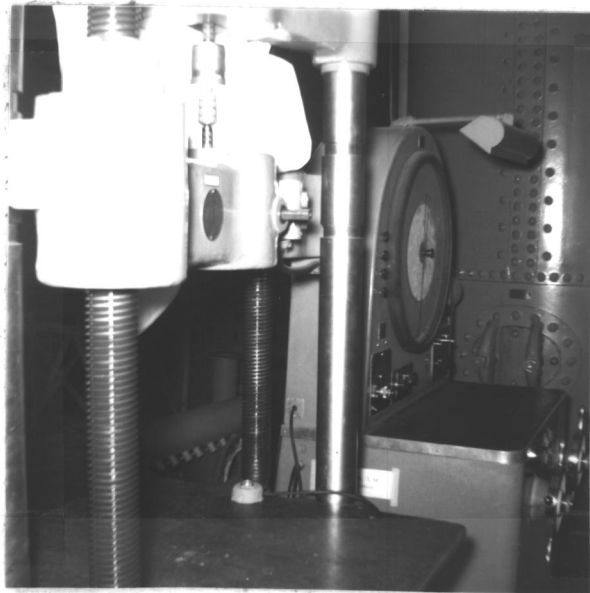
Figure 21.   Universal testing machine
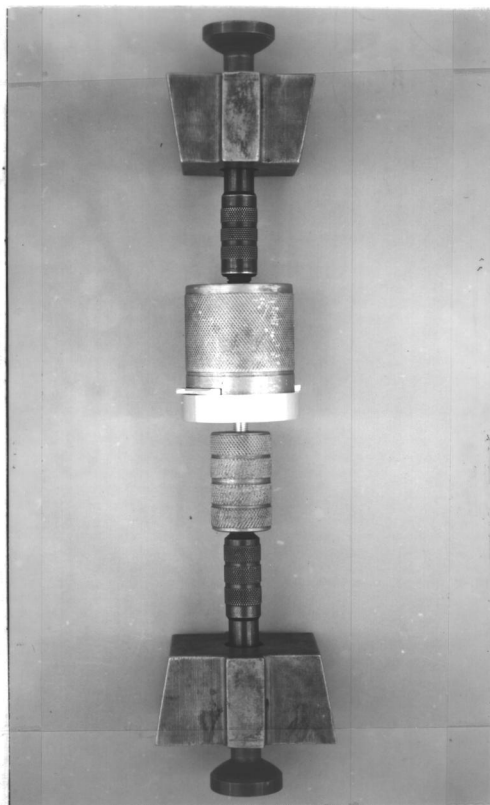
Figure 22.   Clamping fixture for tensile testing

Shaft force-
400 lb/cm

Stud force-
236 lb/cm

Time-5 ms/cm
Figure 23a. Drop
height 1/4 inch

Shaft force-
400 lb/cm

Stud force-
236 lb/cm

Time-5 ms/cm
Figure 23b. Drop
height 1/2 inch

Shaft force-
400 lb/cm

Stud force-
236 lb/cm

Time-5 ms/cm
Figure 23c. Drop
height 3/4 inch

Shaft force-
400 lb/cm

Stud force-
236 lb/cm

Time- 5 ms/cm
Figure 23d. Drop
height 1 inch

Shaft force-
400 lb/cm

Stud force-
236 lb/cm

Time-5 ms/cm
Figure 23c. Drop
height 1-3/8 inch

Figure 23.   Force versus time oscilloscope traces
for various dropping heights of the
drop shaft. Upper is shaft strain
gage; lower is stud strain gage.
(Weighted shaft - 21.4 pounds)

Shaft force-
400 lb/cm

Stud force-
236 lb/cm

Time - 0.5 ms/cm
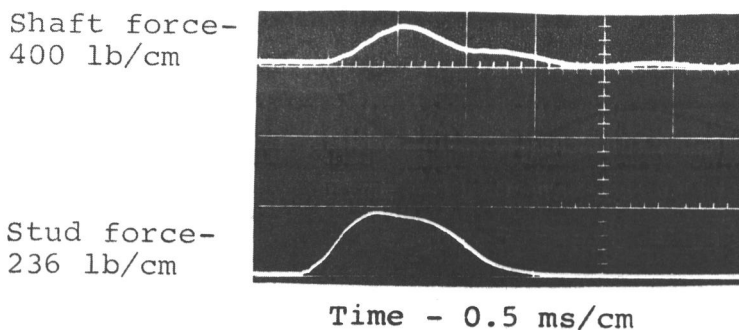
Figure 24a.   **Weighted shaft - 9.1 pounds**

Shaft force-
400 lb/cm

Stud force-
236 lb/cm

Time - 1.0 ms/cm
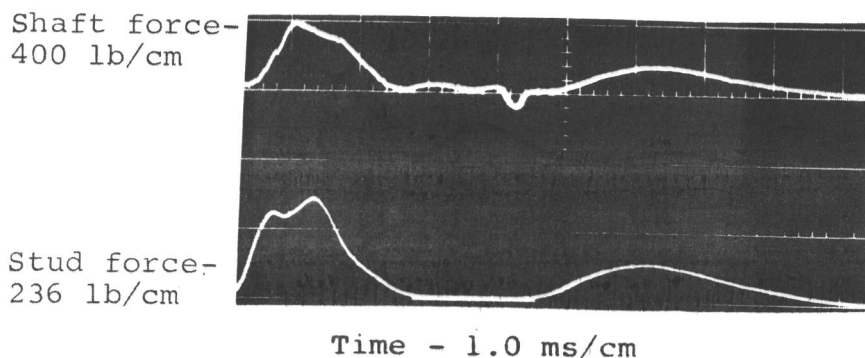
Figure 24b.   **Weighted shaft - 19.7 pounds**

Shaft force-
400 lb/cm

Stud force-
236 lb/cm

Time - 2.0 ms/cm
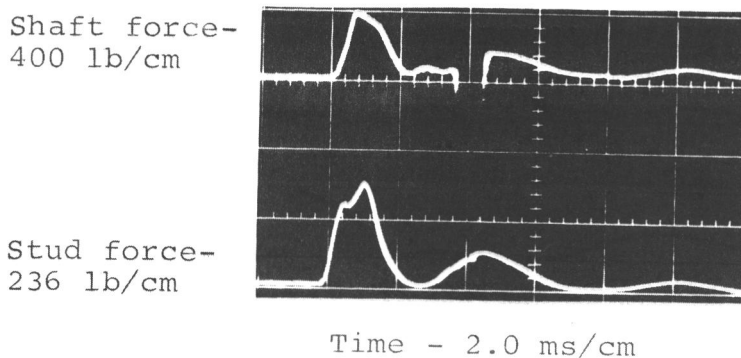
Figure 24c.   Weighted shaft - 24.7 pounds

Figure 24 a-c.   Force vs time oscilloscope traces
                   for various weights
                   (Dropping height - 1-3/8 inches)

Shaft force-
400 lb/cm

Stud force-
236 lb/cm

Time - 2 ms/cm
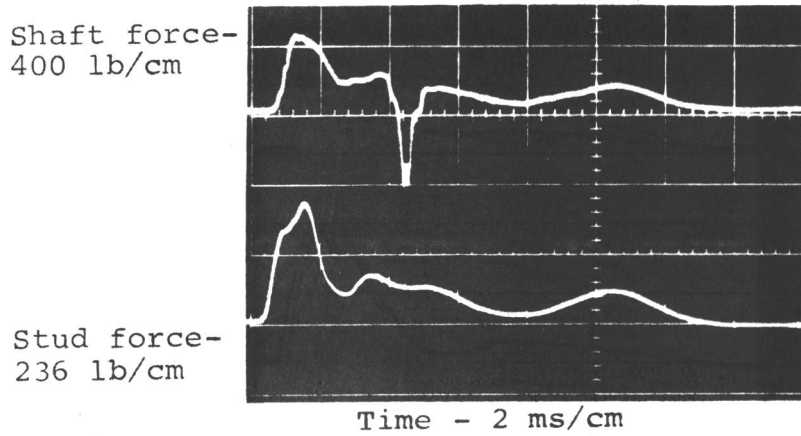
Figure 24d.   Weighted shaft - 34.7 pounds

Shaft force-
400 lb/cm

Stud force-
236 lb/cm

Time - 2 ms/cm
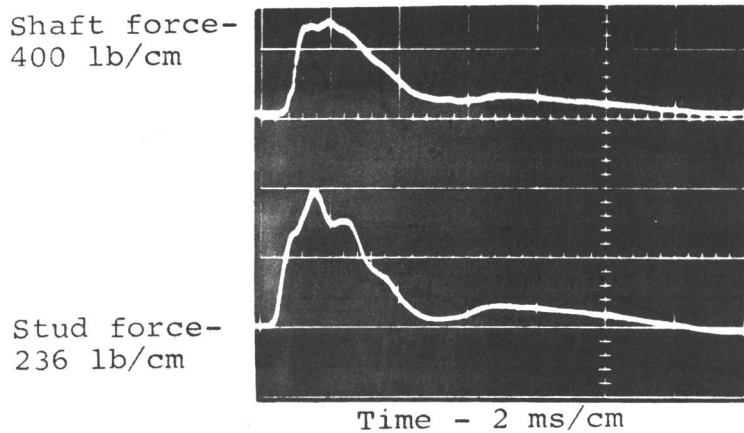
Figure 24e.   Weighted shaft - 39.7 pounds

Figure 24 d-e.   Force vs time oscilloscope traces
for various weights
(Dropping height - 1-3/8 inches)
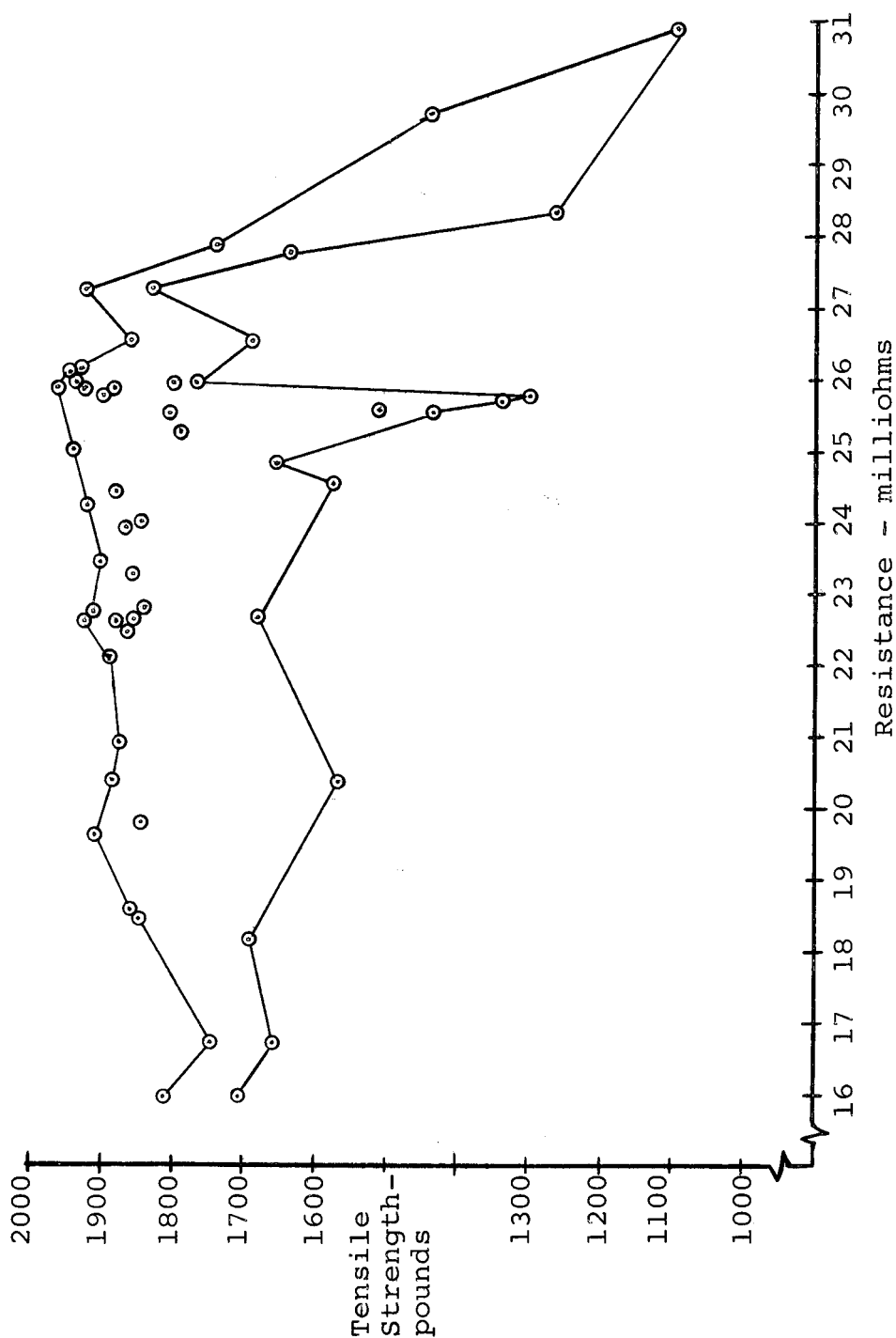
Figure 25.   Tensile strength versus resistance
            (voltage - 150 volts, capacitance - 0.0775
            farads, drop height - 1-3/8 inch,
            weight - 19.7 pounds)

Figure 26, p. 34 shows a typical temperature versus time oscilloscope trace. It is analyzed in the following manner:

1. The arc starts, and the temperature trace is lost due to noise.

2. The arc is extinguished, and temperature trace reappears at a temperature near the vaporization point of aluminum. This is the start of the freeze time period.

3. The thermocouple is being forced into a cooler region of the molten aluminum by the force applied by the stud.

4. The force has reached a maximum value and is starting to decrease.

5. The force is zero and exponential decay of temperature is starting.

6. The molten metal is freezing and the cooling rate is decreased. This is the end of the freeze time period.

7. The metal is again a solid and exponential decay of temperature is again observed.

Figure 27, p. 34 shows the temperature versus time relationship near the 25.6 milliohm resistance point where freeze times of either 2.5 milliseconds or 20 milliseconds were obtained. This figure is a long freeze time case and is analyzed in the following manner:

1. The arc starts, causing r.f. interference and loss of trace.

2. The arc is extinguished and force is applied, temperature drops to near the freeze point. This is the start of the freeze time period.

3. Force removed and the thermocouple is removed from the melt (thermocouple probably separated). A broken thermocouple with both wires in a molten pool works satisfactorily.

4. The thermocouple is back in the melt and the temperature is rising due to the current flowing in a reduced cross-sectional area.

5. The second force application increases the cross-sectional area and the material cools. The freeze point is not shown on this trace, but is estimated to be about 20 milliseconds.

Maintaining the parameter settings used in obtaining the tensile strength versus resistance relationship, data were obtained for the freeze time versus resistance relationship shown in Figure 28. It is to be noted that the freeze times corresponding to 25.6 milliohms resistance were either about 2.5 milliseconds or 20 milliseconds and values between these two limits were not obtained. Since the force waveform was affecting the freeze time, a linearized freeze time versus resistance was approximated as shown by the straight line of Figure 28 and is based on the following.

The short freeze times (less than 3 milliseconds) are dependent on the energy put into the weld zone during the arc period. The freeze times corresponding to resistance values between 25.6 milliohms and 16 milliohms are dependent on the arc period energy plus the tensile force period energy, and are therefore dependent on the force relationships. The freeze times corresponding to

Thermocouple
EMF -
20 mv/cm

1 2 3 4 5   6 7

Time - 5 ms/cm
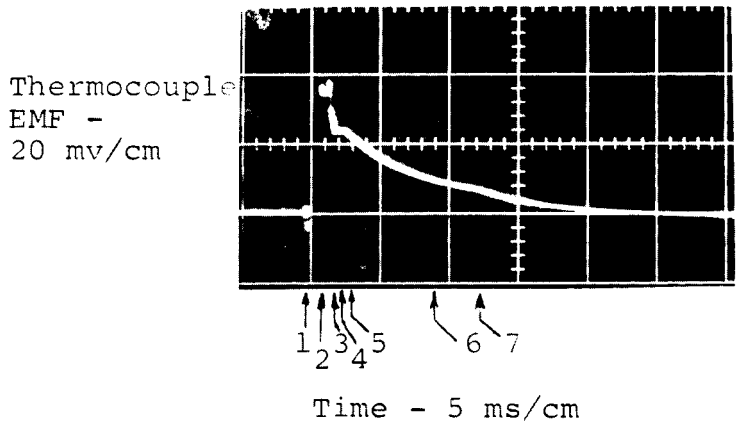
Figure 26.   Typical temperature versus
time curve

Thermocouple
EMF -
10 mv/cm

1 2   3 4   5   Estimated
Freeze Point

Time - 2 ms/cm
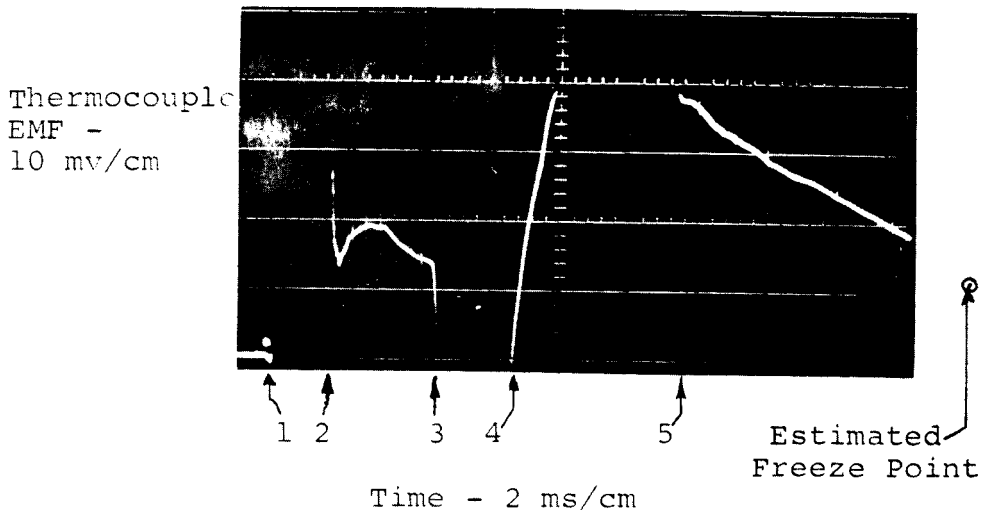
Figure 27.   Temperature versus time curve
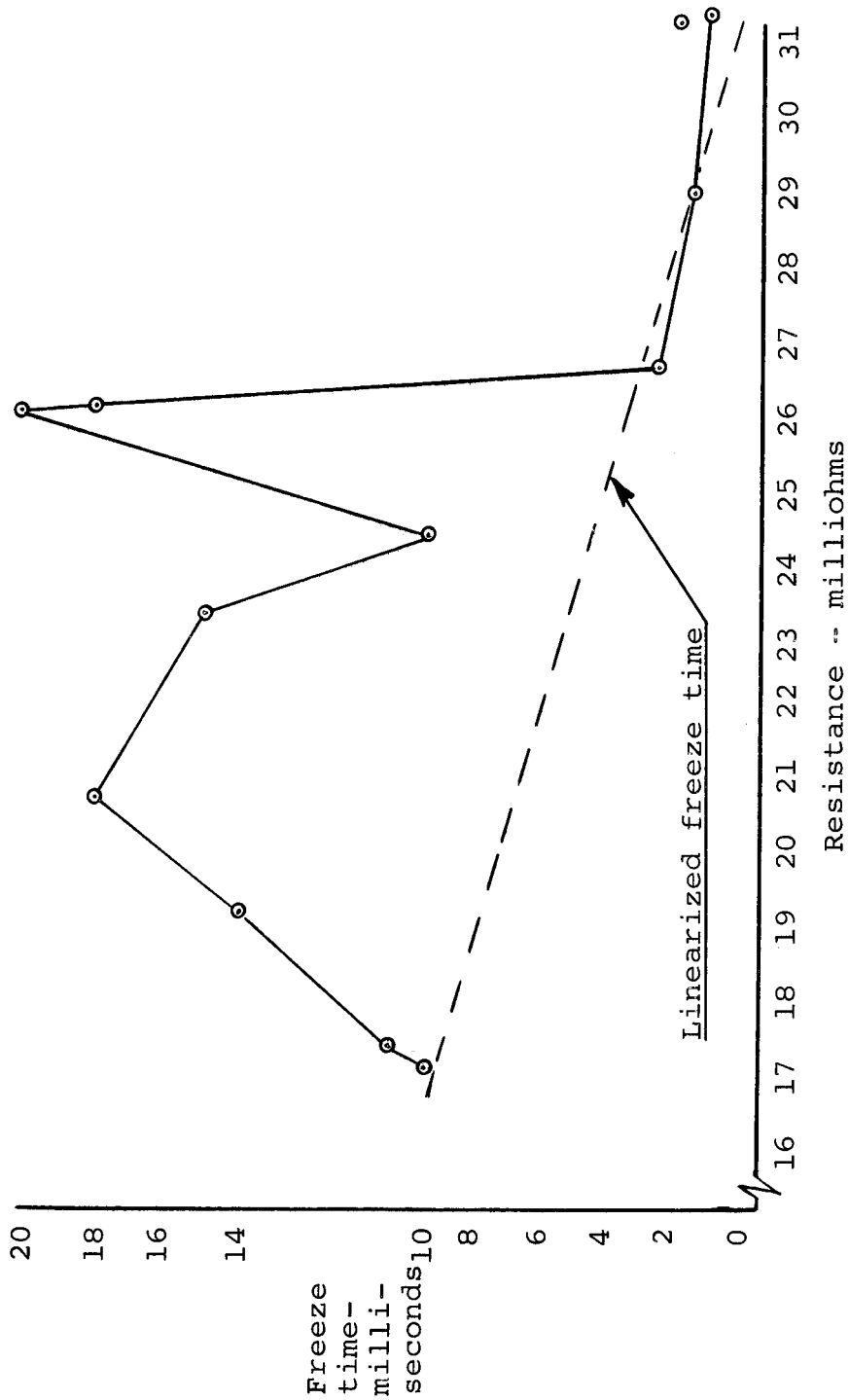
Figure 28. Freeze time versus resistance
(voltage - 150 volts, capacitance 0.0775
farads, drop height - 1-3/8 inches,
weight - 19.7 pounds)

resistance values less than 16 milliohms are apparently
not affected by the tensive force. More metal was melted
during the arc period resulting in adequate conductivity
to limit energy added during the tensile force period.

The tensile strength versus linearized freeze time is
shown in Figure 29, p. 37. The tensile strength versus
linearized freeze time is necessary to have a single
valued function for tensile strength. The values of
tensile strength were found by transforming a freeze time
to a value of resistance (Figure 28) and checking the
tensile strength corresponding to that resistance on
Figure 25.

DISCUSSION OF ORIGINAL DROP SHAFT RESULTS

Any freeze time (freeze time starts at arc out and
ends at the freeze point) occurring during a period of
tensive force results in weak welds. A wide variation of
tensile strength exists for welds made at 25.6 milliohms
resistance. This resistance value corresponds to a
linearized freeze time of approximately three milliseconds.
Three milliseconds is the start of the tensive force as
shown on Figure 24b. A linearized freeze time (three
milliseconds) corresponding to this value of resistance
is a long freeze time (20 milliseconds). The freeze time
may be long enough to cause overaging and hence weaker
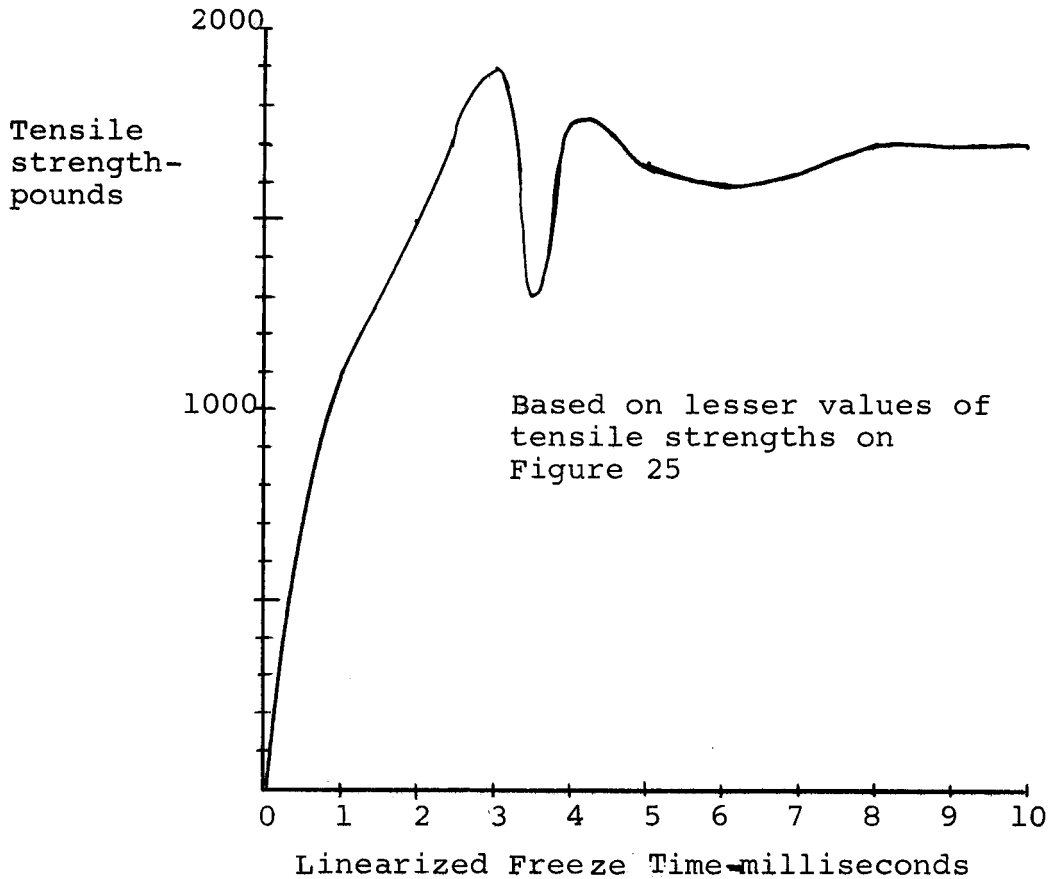
Figure 29. Tensile strength versus linearized
freeze time

(voltage – 150 volts, capacitance 0.0775
farads, weight – 19.7 pounds,
drop height – 1-3/8 inches)

welds. If the tensive force occurs before the freeze time, it is likely that the stud will rise slightly from the plate, and form a reduced diameter molten weld zone. The current through this reduced diameter weld zone may add additional heat energy and raise the temperature as shown in Figure 27. This will cause a thicker weld zone which is characteristically weaker.

The force wave reflections are caused by discontinuities and poor coupling with the air. The wave reflections could have been reduced by using a high-damping-factor material. The force wave reflections are analogous to voltage wave reflections on a short circuited transmission line (1, p. 205). The drop shaft had step discontinuities where the shaft changed from one-half inch diameter to three-fourths inch diameter and where it changed from three-fourths inch diameter to the three inch diameter lead shot container. The last and most severe discontinuity existed where the lead shot container coupled with the air. All of the above discontinuities led to force wave reflections on the drop shaft. The drop shaft is shown in Figure 30. The drop shaft used was placed in the alignment bracket as shown in Figure 31. This caused a slight velocity limiting condition due to the trapped air which escaped through the bearing clearance space.
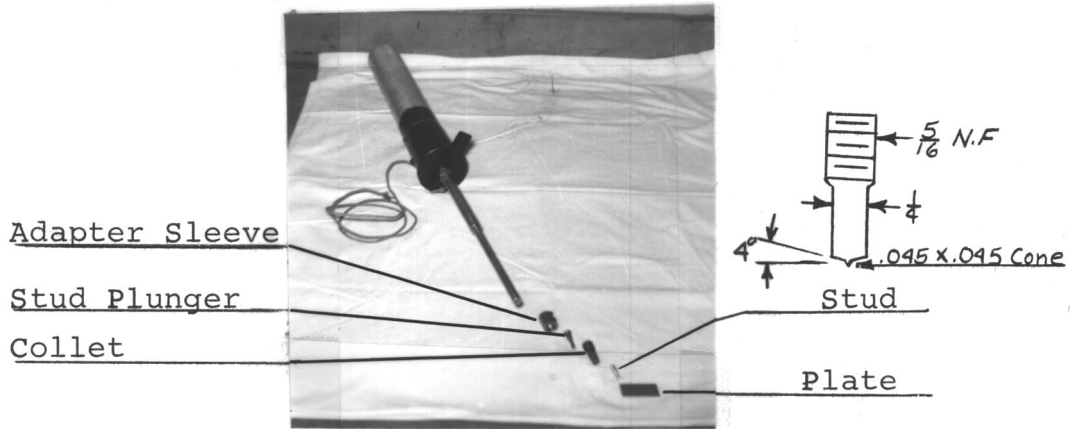
Figure 30. Original drop shaft and hardware
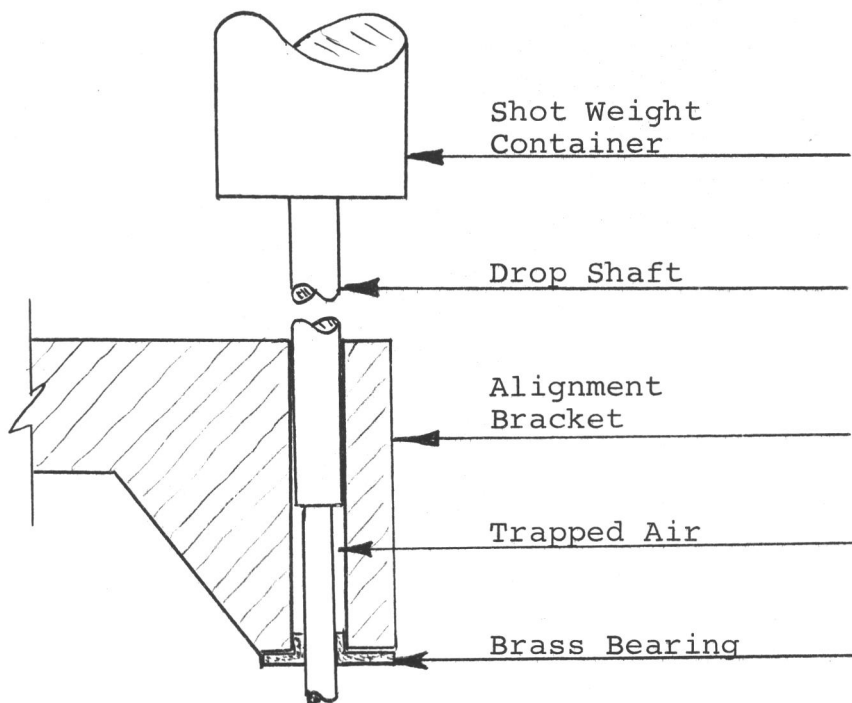
Figure 31. Drop shaft in the alignment bracket

Metallurgical relationships were also observed in a general sense. Overaging occurred if the temperature remained too high for too long a period. If the weld zone was too thick, cracking of the weld zone resulted. In specimens where both thick and thin portions of the weld zone occurred, the thick portion would be cracked and the thin would not be cracked. The cracks were usually perpendicular to the plate (across the weld zone) but cracking, parallel to the plate, occurred in very thick sections (Thin was considered less than three mils; thick, greater than three mils; and very thick, greater than eight mils). The cracking was due to the thermal coefficient of expansion and solidification shrinkage (2, p. 13, 810).

DESIGN OF EXPONENTIAL DROP SHAFT

An exponential drop shaft was designed to eliminate wave reflections observed in Figure 24, p. 29, 30. The existence of a tensive force wave with the original drop shaft, at the time of freeze, resulted in poor quality welds. The design criteria were based on smooth transitions, high damping and coupling of the energy into the air. The exponential drop shaft is shown in Figure 32 and the drawing is on page 59 of the appendix.

Mild steel was selected for the drop shaft material. This was readily available and has a much higher damping factor than the brass previously used (16, ch. 8)(2, p.910).
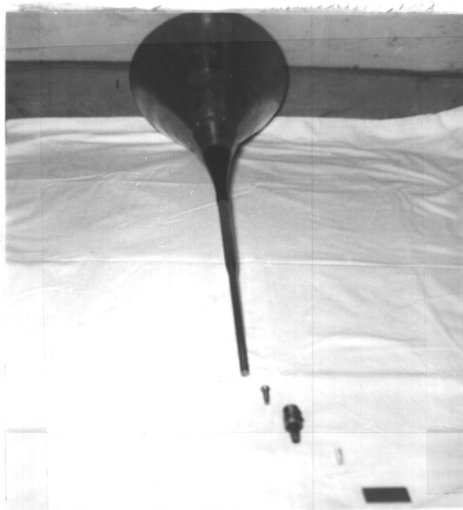
Figure 32.   Exponential drop shaft

Nickel and grey cast iron have higher damping factors,
but nickel was not readily available and grey cast iron
is brittle. Mild steel has a higher modulus of elastic-
ity than brass and results in a greater magnitude of
force for a shorter period of time.

Smooth flowing transitions are required to help
eliminate wave reflections. This was considered in making
the drop shaft transition from three-fourths inch to one-
half inch and for the stud plunger which fits between the
stud and the one-half inch diameter section of the drop
shaft.

Coupling of the energy into the air was the most im-
portant consideration, since the main-reflection period
showed a discontinuity at the end of the original shaft.
The old victrola phonographs, automobile horns, and musical
wind instruments probably are the most efficient examples
of coupling energy into the air, therefore an exponential

type horn was designed into the top of the new drop shaft.

Since the maximum value of force should be variable, it was conceived that lead shot with its inherent high damping could be satisfactorily added to the horn. This probably will not affect the coupling to the air signifi-cantly since the air between the shot will still be placed in motion.

The trapped air was relieved to reduce velocity limiting. After the exponential drop shaft was fitted and aligned in the bracket, four holes (one-sixteenth diameter) were drilled just above the alignment bracket's one-half inch bearing. This was necessary since the clearance of the new shaft was less than two mils on the diameter.

RESULTS OF THE EXPONENTIAL DROP SHAFT MEASUREMENTS

Force versus time oscillograms for varying weight are shown in Figure 33. No wave reflections were observed, just the force impulse shown. This type of force trace should result in a thin weld zone provided the stud tip design is such that the solid surfaces of the stud and plate nearly mate after the arc is extinguished.

A few welds were tensile tested and the data is on page 60 of the appendix. Welding of dissimilar metal combinations were made using the same tip design. When brass or steel studs were used, the tip could not be

Stud force-
221 lb/cm
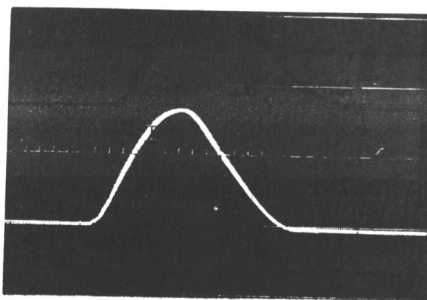
Time - 0.5 ms/cm

Figure 33a.   Drop weight - 8 pounds

Stud force-
221 lb/cm
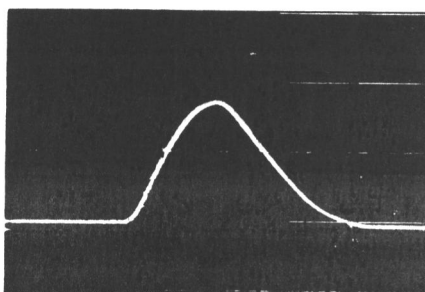
Time - 0.5 ms/cm

Figure 33b.   Drop weight - 9.2 pounds

Stud force-
222 lb/cm
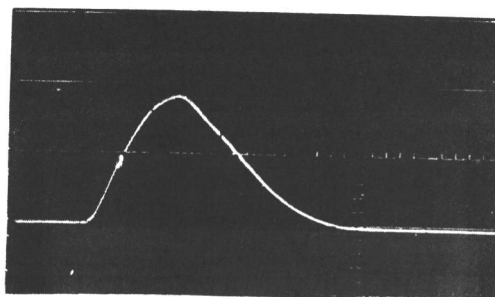
Time - 0.5 ms/cm

Figure 33c.   Drop weight - 11.5 pounds

Figure 33 a-c.   Force versus time for exponential drop
shaft, with various weights.

Stud force-
226 lb/cm
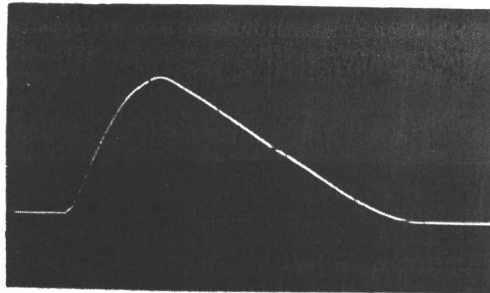
Time - 0.5 ms/cm

Figure 33d.   Drop weight - 16.3 pounds

Stud force-
226 lb/cm
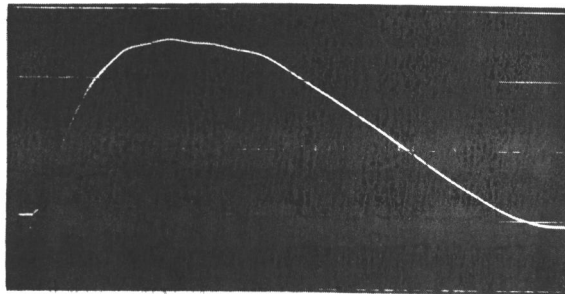
Time - 0.5 ms/cm

Figure 33e.   Drop weight - 36.2 pounds

Stud force-
226 lb/cm
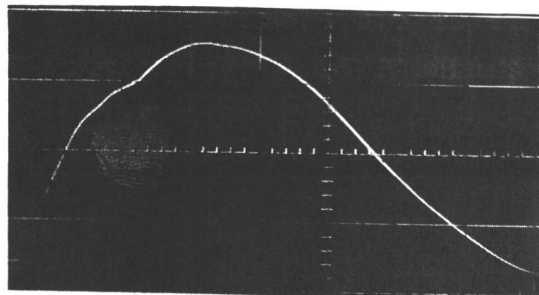
Time - 0.5 ms/cm

Figure 33f.   Drop weight - 57.7 pounds

Figure 33 d-f.   Force versus time for exponential
drop shaft with various weights

melted in the process and incomplete weld area was obtained.
The results of dissimilar welding are outlined in Table I.

Possible	Not Likely
Brass to Copper	6061-T6 Aluminum to Copper
Brass to Steel	6061-T6 Aluminum to Brass
Steel to Copper	6061-T6 Aluminum to Steel

Table I.   Dissimilar-metal welding summary

DISCUSSION OF EXPONENTIAL DROP SHAFT RESULTS

The exponential drop shaft did eliminate wave reflec-
tions, but the welds were filled with voids believed to be
due to high current flow after the arc was extinguished.
The force wave forms were similar as weight was added and
this is an improvement over the original drop shaft.
While preparing for Comstock's experiment, maximum weld
strength resulted using the weight and height combina-
tions of Figure 24e, page 30. This indicates that a
maximum percussive force is needed and a constant force,
after the percussive force, is needed during the freeze
time.

CONCLUSIONS

Tensile strength is a primary function of force and freeze time. The force is a function of weight, height and drop shaft configuration. The temperature characteristics are a function of capacitance, voltage, and circuit resistance. Velocity was not considered but velocity and the stud-tip length control the arc time and hence the amount of energy for any particular voltage, capacitance, and resistance setting.

The oscilloscope measurements of force and temperature are very useful. The measurements allow observation of the force during freeze time. Temperature measurements of 2100 degrees centigrade occurring for less than a millisecond are uncommon but have the same characteristics as slower measurements.

The elimination of process variables was very necessary to observe the force and temperature relationships. The magnetic shielding of the weld zone resulted in a much broader operating range than observed before. The resistance control allowed repeatable results. The oxide layer is still a problem, but polishing with emery paper may remove this variable.

The wave reflections on the drop shaft cause a

variable force wave with weight and can be eliminated by using proper design criteria. The exponential drop shaft eliminated wave reflections but was not characterized by a constant force following the percussive force.

RECOMMENDATIONS

Design a force system which will allow a high percussive force to mate the solidus surfaces of the stud and plate and provide a constant force during freeze time. The exponential drop shaft would provide this characteristic if enough weight (200 pounds) were added, but this is impractical. A force system using hydraulic or pneumatics would be practical and a proposed design is shown on page 61 of the appendix. The proposed design would use high damping materials, provide coupling to the fluid, and have an accumulator built into the force cylinder.

Build a resistor that would be temperature and contact insensitive. Stainless steel is a high resistance material (resistivity about 60 times copper's) and works nicely, except during a high welding rate it heats and changes resistance. By placing the resistor in an oil filled container (temperature controlled by heating) the resistor would be temperature insensitive. Bolt terminals to the resistor at one-half milliohm steps and bring the terminals through the container in a manner similar to a capacitor terminal. All bolted connections should be silvered to reduce contact resistance. This would provide a temperature and contact insensitive resistor.

BIBLIOGRAPHY

1. Albert, Arthur Lemuel. Electrical communication. 3d ed. New York, Wiley, 1957. 593p.

2. American Society for Metals. Metals handbook. Novelty, Ohio, 1948. 1332p.

3. American Society for Metals. Metals handbook 1955 supplement. Cleveland, Ohio, 1955. 208p.

4. American Society for Metals. Metals handbook. 8th ed. vol 1. Metals Park, Ohio, 1961. 1300p.

5. Blood, H. P. Stud welding system speeds curtain wall production. Modern Metals 16: 88-89. Nov. 1960.

6. Brick, R. M. and Arthur Phillips. Structure and properties of alloys. 2d ed. New York, McGraw-Hill, 1949. 485p.

7. Chemical Rubber Co. Handbook of chemistry and physics. 44th ed. Cleveland, Ohio, 1963. 3604p.

8. Corcoran, George F. and Henry R. Reed. Introductory electrical engineering. New York, Wiley, 1957. 527p.

9. Coyne, J. C. Monitoring the percussive welding process for attaching wire to terminals. The Bell System Technical Journal 42: 55-78. 1963.

10. Davis, Harmer E., et. al. The testing and inspection of engineering materials. 2d ed. New York, McGraw-Hill, 1955. 431p.

11. Guy, Albert G. Elements of physical metallurgy. Reading, Massachusetts, Addison-Wesley, 1951. 296p.

12. Heindlhofer, Kalman. Evaluation of residual stress. New York, McGraw-Hill, 1948. 196p.

13. Jakob, Max and George A. Hawkins. Elements of heat transfer. 3d ed. New York, Wiley, 1958. 309p.

14. Kleis, John. Welding dissimilar metals - try percussion welding. Welding Design and Fabrication 35: 34-35. Aug. 1962.

15. Kraus, John D. Electromagnetics. New York, McGraw-Hill, 1953. 604p.

16. Marin, Joseph. Mechanical behavior of engineering materials. Englewood Cliffs, N. J., Prentice-Hall, 1962. 491p.

17. McAdams, William H. Heat transmission. 2d ed. New York, McGraw-Hill, 1942. 459p.

18. Milne, William Edmund. Numerical calculus. Princeton, N. J., Princeton University Press. 393p.

19. Mintz, Max M. Stud welding - precision location without distortion. Tool Engineer 43: 81-82. July, 1959.

20. Perry, Charles C. and Herbert R. Lissner. The strain gage primer. New York, McGraw-Hill, 1955. 281p.

21. Popov, E. P. Mechanics of materials. Englewood Cliffs, N. J., Prentice-Hall, 1952. 441p.

22. Owczarski, W. A. and A. J. Palmer. Percussive welding does the finest work. American Machinist/ Metalworking Manufacturing 105:114. June 12, 1961.

23. Singleton, Robert C. The growth of stud welding. Welding Engineer 48:27-31. July, 1963.

24. Tektronix, Inc. High gain, differential calibrated D. C. preamp type D - Instruction manual. Portland, Oregon. 6p.

APPENDIX

Tungsten Five Percent Versus Tungsten 26 Percent Rhenium

Temperature/emf Data

Temperature Degrees Centigrade	EMF Millivolts
17.78	0.
93.33	1.251
204.44	3.043
315.56	5.044
426.67	7.130
537.78	9.259
648.89	11.410
760.00	13.561
871.11	15.676
982.22	17.747
1093.30	19.749
1204.4	21.725
1315.6	23.632
1426.7	25.428
1537.8	27.100
1648.9	28.832
1760.00	30.471
1871.1	31.905
1982.2	33.354
2093.3	34.587
2204.4	35.919
2315.5	36.869

Manufactured by: Hoskins Manufacturing Company
4445 Lawton Avenue
Detroit 8, Michigan

Residual Stress Measurement

FIRST SPECIMEN - WELD ZONE DATA

Column No.	Weld Zone Thickness	Column No.	Weld Zone Thickness
1	567	11	599
2	456	12	567
3	555	13	688
4	611	14	716
5	724	15	
6	781	16	
7	810	17	876
8	775	18	558
9	727	19	530
10	712		

FIRST SPECIMEN - SPACING DATA
and STRAIN CALCULATIONS

Measurements between indentations of the columns were summed before and after stress relief. Only the summations are displayed, since the individual measurements would be quite voluminous.

Column No.	Summation before stress relief LO	Summation after stress relief Ll	Change in length due to stress relief LO-Ll	Strain $\frac{LO-Ll}{LO}$
1	9664	9648	16	0.001655
2	9626	9630	-4	-0.000416
3	9562	9523	39	0.00408
4	9710	9727	-17	-0.00175
5	9756	9750	+6	0.000615
6	9709	9711	-2	-0.000206
7	9708	9704	4	0.000412
8	9706	9693	13	0.00134
9	9948	9933	15	0.00151
10	9822	9821	+1	+0.00102
11	9686	9712	-26	-0.002683
12	9790	9847	-57	-0.00583
13	9924	9943	-19	-0.001915
14	9748	9778	-30	-0.00308
15	9449	9485	-36	-0.00381
16	9808	9818	-10	-0.00102
17	9761	9797	-36	-0.00369
18	9639	9637	2	0.000208
19	9880	9905	-25	-0.00253

Figure 19 depicts this data graphically

Least Squares Approximation - First Specimen

Only the coefficients are tabulated (18, p. 242-249)
and are functions of the location given by the column
numbers. The following is for strain and must be
divided by 1000 to yield correct results:

$S_O = 19$; $S_1 = 190$; $S_2 = 2470$; $S_3 = 36,100$;

$S_4 = 562,666$; $S_5 = 9,133,300$; $S_6 = 152,455,810$;

$V_O = 16.09$; $V_1 = -302.718$; $V_2 = -4775.268$;

$V_3 = -73,272.29$

$$S_O\ ao + S_1\ a_1 + S_2\ a_2 + S_3 a_3 = V_O$$

$$S_1\ ao + S_2 a_1 + S_3 a_2 + S_4 a_3 = V_1$$

$$S_2\ ao + S_3 a_1 + S_4 a_2 + S_5 a_3 = V_2$$

$$S_3\ ao + S_4 a_1 + S_5 a_2 + S_6 a_4 = V_3$$

Solving the above for ao, a_1, a_2, a_3 yields the
following approximate solution for strain:

Strain = $(-0.954 + 1.23r -0.192r^2 + 0.00677r^3)/1000$

r	Strain
1	.00009
3	.00119
6	.000974
9	-.000501
12	-.00243
15	-.00191
18	-.000585

Residual Stress Measurement

SECOND SPECIMEN - WELD ZONE DATA

Column No.	Weld Zone Thickness	Column No.	Weld Zone Thickness
Outside Diam.	750	12	670
1	500	13	550
2	400	14	500
3	400	15	510
4	360	16	460
5	390	17	540
6	425	18	570
7	495	19	430
8	600	Center of Stud	280
9	670		
10	760		
11	710		

SECOND SPECIMEN - SPACING DATA and STRAIN CALCULATIONS

Measurements between indentations of the columns were summed before and after stress relief. Only the summations are displayed, since the individual measurements would be quite voluminous.

Column No.	Summation before stress relief LO	Summation after stress relief L1	Change in length due to stress relief LO-L1	Strain $\frac{LO-L1}{LO}$
1	9943	9945	-2	-0.000201
2	9984	10003	-19	-0.00191
3	9854	9884	-30	-0.00304
4	9970	9985	-15	-0.00151
5	9925	9894	31	0.00312
6	9840	9858	-18	-0.00183
7	10122	10120	2	0.000197
8	9889	9892	-3	-0.000304
9	10034	10018	16	0.00155
10	10015	10025	-10	-0.000997
11	10039	10036	3	0.000299
12	10019	10006	13	0.00130
13	10015	9996	19	0.00189
14	10054	10044	10	0.000995
15	10048	10036	12	0.00119
16	10075	10072	3	0.000298
17	10068	10043	25	-0.00248
18	10073	10075	-2	-0.000199
19	10052	10053	-1	-0.0000995

Figure 20 depicts this data graphically

Least Squares Approximation - Second Specimen

The values for S_o, S_1, ... S_6 are the same as the first specimen, and V_o = 3.2285, V_1 = 105.05; V_2 = 1670.0 and V_3 = 24,948.

Solving the same set of equations as before, with the new values of V_i, the following approximate solution for strain is obtained:

Strain = $(-.263 - .769r + .131r^2 - .00489r^3)/(1000)$

r	Strain
1	-.000906
3	-.001523
6	-.001217
9	-.000138
12	+.000925
15	+.001173
18	-.000179

Tensile Strength versus Resistance Data

Voltage = 150 volts,   Capacitance = 77,500 microfarads,

Weight = 19.7 pounds,   Drop Height = 1-3/8 inches.

Resistance-milliohms	Tensile Strength-pounds	Resistance-milliohms	Tensile Strength-pounds
15.96	1705	25.00	1940
15.96	1810	25.21	1790
16.67	1655	25.51	1435
16.67	1750	25.51	1805
18.16	1690	25.56	1510
18.48	1850	25.67	1900
18.53	1855	25.67	1900
19.60	1915	25.70	1340
19.73	1845	25.82	1880
20.35	1565	25.88	1930
20.35	1885	25.89	1965
20.87	1875	25.91	1800
22.10	1890	25.93	1940
22.45	1865	25.95	1770
22.58	1880	26.02	1945
22.58	1925	26.09	1930
22.62	1855	26.47	1860
22.65	1680	26.52	1690
22.72	1915	27.23	1830
22.75	1840	27.26	1925
23.26	1855	27.75	1635
23.41	1900	27.84	1740
23.90	1865	28.28	1265
23.95	1845	29.68	1440
24.19	1920	30.90	1090
24.44	1885	32.14	875
24.48	1575	34.14	315
24.82	1655		

Freeze Time versus Resistance Data

Voltage = 150 volts,   Capacitance = 77,500 microfarads,

Weight = 19.7 pounds,   Drop Height = 1-3/8 inches.

Resistance	Freeze Time
15.96	9 ms
17.16	11 ms
18.99	14 ms
20.65	18 ms
22.55	15 ms
24.16	9 ms
25.67	20 ms
25.70	18 ms
26.69	2.8 ms
28.75	1.9 ms
31.00	2.4 ms
30.96	2.0 ms
31.07	1.4 ms

12" top diameter
60° cone bolted
with 6 #10 machine
screws to the shaft
3.30

2.56

2.00

1.56

1.23

0.95

0.748

Notes: 1. All dimensions
are inches
2. ✔ marked surfaces
are finished
3. x marked surfaces
are rough
4. Material-mild
steel

0.748

0.498

0.498

Lead shot
container

0.5

1.0

1.0

1.0

1.0

1.0

1.0

1.0

1.0

8.0
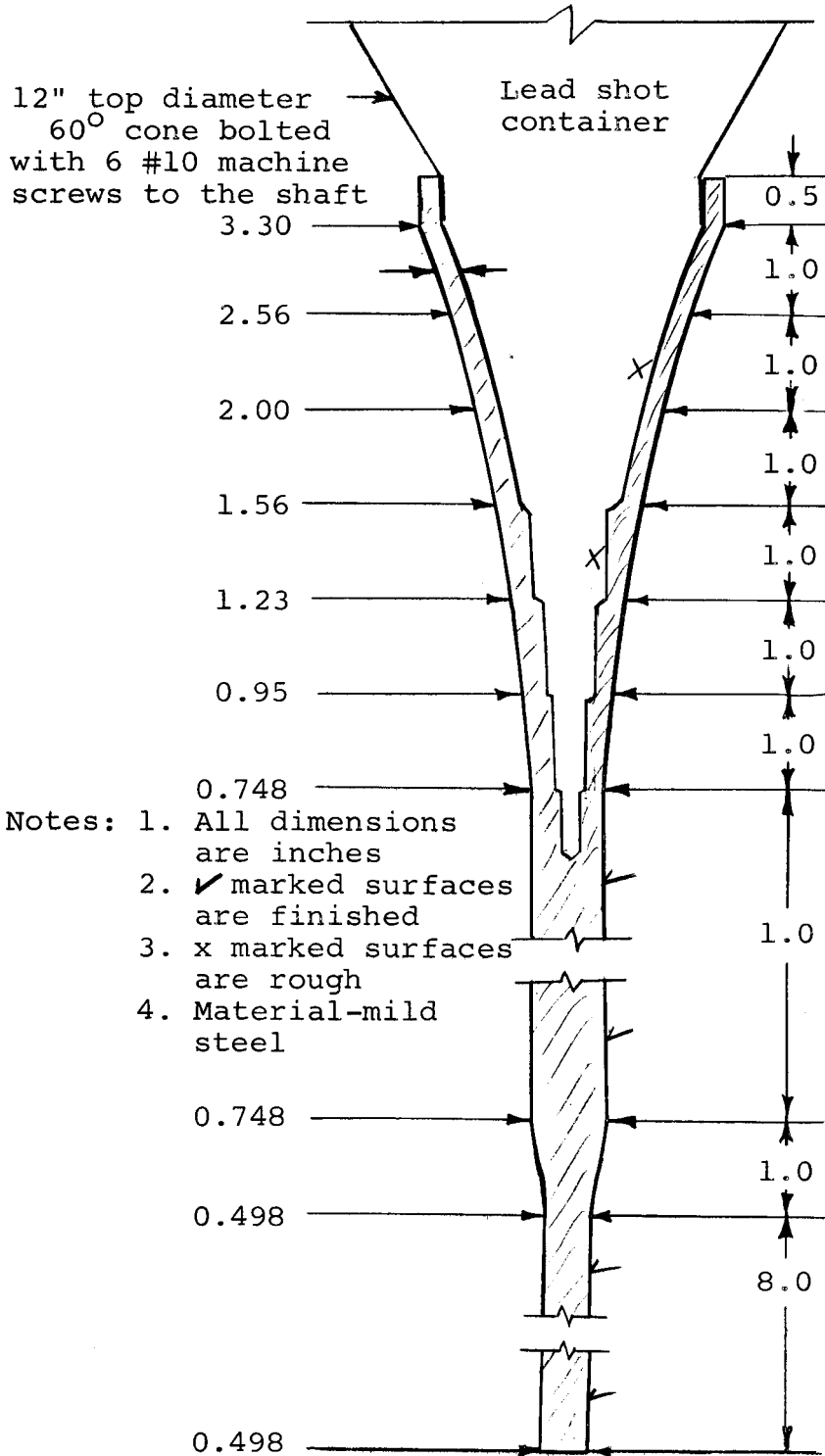
Exponentially-shaped Drop Shaft Design

EXPONENTIAL DROP SHAFT DATA

Height-inches	Weight-pounds	Voltage-volts	Capacitance-farads	Resistance-milliohms	Tensile Strength-pounds
1.0	42.7	130	0.0775	18.77	1620
"	"	140	"	"	1842
"	"	145	"	"	1625
"	"	150	"	"	1770
"	"	155	"	"	1545
"	"	160	"	"	1605
"	"	170	"	"	1735
"	"	180	"	"	1775
"	"	190	"	"	1745
"	"	200	"	"	1700
"	26.2	140	"	"	1390
"	31.2	"	"	"	1760
"	36.2	"	"	"	1765
"	41.2	"	"	"	1870
"	46.2	"	"	"	1625
"	51.2	"	"	"	1470
"	57.7	"	"	"	1785
"	41.2	"	"	19.00	1625
"	"	"	"	17.92	1770
"	"	"	"	15.77	1840
"	"	"	"	19.91	1125
"	"	"	"	21.7	1240
"	"	"	"	17.07	1675
"	"	"	"	17.03	1905
"	"	"	"	17.00	1825
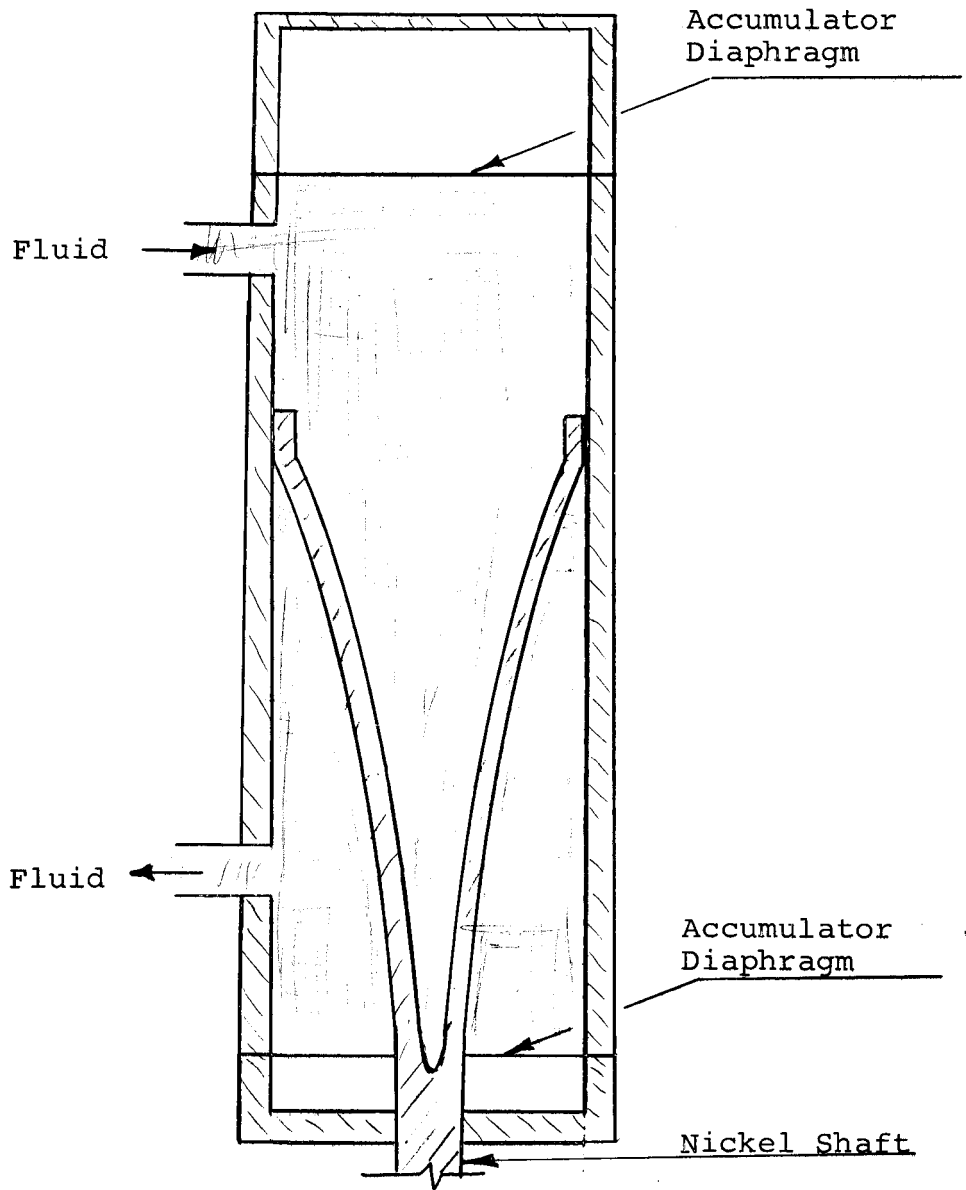
Proposed Force System

Original Drop Shaft Resonant Frequency and Wave Period
Calculations.

A calculation for the brass shaft (assuming one end
fixed and neglecting the shot container) indicated a
resonant frequency of 6000 cycles per second. Since the
shaft is not connected solidly to the welded stud
(collet connection), the period for the wave to travel
to the discontinuity and back to the stud is more
realistic. The periods for various force system com-
ponents is calculated below.

$$*\text{Brass Shaft Period} = \frac{3 \text{ feet}}{11,400 \text{ feet per second}} = .26 \text{ milli-seconds}$$

$$\text{Aluminum Shot Container Period} = \frac{4 \text{ feet}}{16,300 \text{ feet per second}} = .26 \text{ milliseconds}$$

$$\text{Hypothetical Lead Column Period} = \frac{4 \text{ feet}}{6,000 \text{ feet per second}} = .6 \text{ milliseconds}$$

*Approximate velocities were used (7, p2597)

Due to unavailability of velocities for lead shot,
actual system period calculations were not performed.
However, it is to be noted in Figure 24 that the period
becomes longer as more shot is added.